
Article:
Gray, H.J., Tucker, G.E., Mahan, S.A. et al. (2 more authors) (2017) On extracting sediment transport information from measurements of luminescence in river sediment. Journal of Geophysical Research: Earth Surface. ISSN 2169-9011

https://doi.org/10.1002/2016JF003858

AGU PUBLICATIONS

JGR

Journal of Geophysical Research: Earth Surface

RESEARCH ARTICLE
10.1002/2016JF003858

Key Points:
- We develop a model coupling transport of fine sand and luminescence to explain the patterns of luminescence observed in river sediment
- The model successfully reproduces the patterns of luminescence measurements in two river systems
- Best fit values from the model describe sediment transport for fine sand, although our observed range is broader than previous studies

Supporting Information:
- Supporting Information S1

Correspondence to:
H. J. Gray,
harrison.gray@colorado.edu

Citation:
Gray, H. J., G. E. Tucker, S. A. Mahan, C. McGuire, and E. J. Rhodes (2017), On extracting sediment transport information from measurements of luminescence in river sediment, *J. Geophys. Res. Earth Surf.*, *122*, doi:10.1002/2016JF003858.

Received 12 FEB 2016
Accepted 23 FEB 2017
Accepted article online 2 MAR 2017

On extracting sediment transport information from measurements of luminescence in river sediment

Harrison J. Gray[1,2], Gregory E. Tucker[1], Shannon A. Mahan[2], Chris McGuire[3], and Edward J. Rhodes[3,4]

[1]Cooperative Institute for Research in Environmental Sciences and Department of Geological Sciences, University of Colorado Boulder, Boulder, Colorado, USA, [2]U.S. Geological Survey Luminescence Geochronology Laboratory, Denver Federal Center, Denver, Colorado, USA, [3]Department of Earth, Planetary, and Space Sciences, University of California, Los Angeles, California, USA, [4]Department of Geography, University of Sheffield, Sheffield, UK

Abstract Accurately quantifying sediment transport rates in rivers remains an important goal for geomorphologists, hydraulic engineers, and environmental scientists. However, current techniques for measuring long-time scale (10^2–10^6 years) transport rates are laborious, and formulae to predict transport are notoriously inaccurate. Here we attempt to estimate sediment transport rates by using luminescence, a property of common sedimentary minerals that is used by the geoscience community for geochronology. This method is advantageous because of the ease of measurement on ubiquitous quartz and feldspar sand. We develop a model from first principles by using conservation of energy and sediment mass to explain the downstream pattern of luminescence in river channel sediment. We show that the model can accurately reproduce the luminescence observed in previously published field measurements from two rivers with very different sediment transport styles. The model demonstrates that the downstream pattern of river sand luminescence should show exponential-like decay in the headwaters which asymptotes to a constant value with further downstream distance. The parameters from the model can then be used to estimate the time-averaged virtual velocity, characteristic transport lengthscale, storage time scale, and floodplain exchange rate of fine sand-sized sediment in a fluvial system. The sediment transport values predicted from the luminescence method show a broader range than those reported in the literature, but the results are nonetheless encouraging and suggest that luminescence demonstrates potential as a sediment transport indicator. However, caution is warranted when applying the model as the complex nature of sediment transport can sometimes invalidate underlying simplifications.

1. Introduction

The rate of suspended sediment transport by rivers is a key variable in understanding the evolution of landscapes [*Tucker and Hancock*, 2010], the behavior of rivers [*van Rijn*, 1993], the lifespan of reservoirs [*Syvitski et al.*, 2005; *Papanicolaou et al.*, 2008], and the impacts of development on sedimentation [*Syvitski et al.*, 2005]. Surprisingly, we have little ability to quantify suspended sediment transport rates over long (10^2–10^6) time scales beyond hard-to-constrain analytical models, time-consuming tracer experiments, and field-intensive sediment budgeting studies [*Haschenburger and Church*, 1998; *Martin and Church*, 2004; *Bradley and Tucker*, 2012, and references therein]. This knowledge gap reflects a lack of reliable field data with which to calibrate models, and uncertainties in the travel velocities and exchange rates of various grain sizes throughout a river system [*Papanicolaou et al.*, 2008]. For this reason, it is important to explore possible connections between geomorphic process and material properties of sediment that may act as a proxy for these processes.

One such material property, luminescence, exhibits systematic downstream variations within river systems, and these variations may provide a means to obtain information on sediment transport. Luminescence arises as a property of minerals where bonding electrons excited by ionizing radiation become trapped in defects in a mineral's crystal lattice [*Rhodes*, 2011]. The trapped electrons occupy energy levels between the valence and conduction bands and remain stable until a source of energy such as heat or sunlight gives the electrons the energy needed to escape the trap, releasing photons in the process. [*Rhodes*, 2011]. The emission of these photons due to energy from visible light is termed optically stimulated luminescence

(OSL) [*Huntley et al.*, 1985]. A new method developed for potasssium-feldspar minerals uses infrared light at a series of elevated temperatures and is termed post-infrared infrared stimulated luminescence (post-IR IRSL) [*Thomsen et al.*, 2008; *Buylaert et al.*, 2009]. When pIRIR is measured at a series of elevated temperatures, different luminescence signals can be measured by a technique known as multiple-elevated-tempurature post-infrared infrared (MET-pIRIR) stimulated luminescence [*Li and Li*, 2011]. The measurement of luminescence has been exploited as a geochronometer by the geoscience community, as common minerals such as quartz and feldspar can have trapped electrons removed by exposure to sunlight in a process known as bleaching. This resetting by light exposure, and the subsequent buildup of luminescence due to background ionizing radiation when a mineral grain is buried, allows the determination of the elapsed time since last light exposure, which is taken to be equivalent to a depositional age [*Huntley et al.*, 1985].

The downstream variation in luminescence of in-channel fluvial fine sand (90–250 μm grain size) has been documented in two studies. *Stokes et al.* [2001] observed that the equivalent dose of quartz OSL of sediment in the Loire River, France, displayed an overall decrease in luminescence with downstream distance from the river source. *McGuire and Rhodes* [2015a], using an MET-pIRIR protocol, noted that the equivalent dose for various measurement temperatures also demonstrated a general decrease with downstream distance for the Mojave River in Southern California. Despite the striking difference in fluvial characteristics between the sites, the two studies revealed similar patterns: in both cases, luminescence tended to decrease downstream, at a rate that also decreased downstream. Furthermore, none of the samples collected showed complete bleaching, even though the sampled sediment was clearly subject to transport. The observed downstream decline of luminescence signal has been interpreted as a consequence of progressive bleaching during transport [*Jain et al.*, 2004; *Gray and Mahan*, 2015]. While such an interpretation seems logical, it leaves several questions unanswered. What factors govern the rate of bleaching with respect to transport distance? Why does sand sampled from channel deposits retain a signal even when the material is clearly subject to contemporary transport? To what extent do variations in luminescence along a river reflect transport dynamics, such as the rate of channel-floodplain exchange or the virtual velocity of grains?

To attempt to explain this downstream decrease in residual luminescence, or "zero age" luminescence, we introduce a mathematical model, which is similar to those for open channel flow and tracer transport [*Lauer and Parker*, 2008a; *Lauer and Willenbring*, 2010; *Pizzuto et al.*, 2014], that describes the space-time evolution of quartz and feldspar luminescence signals in fluvial suspended sand. The model is then used to address three objectives. First, we compare model predictions with the data sets of *Stokes et al.* [2001] and *McGuire and Rhodes* [2015a, 2015b] in order to determine whether the model provides a consistent explanation for their observations. Second, we assess whether such a model, when fit to along-stream observations of luminescence, holds the potential to provide information about rates and patterns of sediment transport. The third aim is to determine whether preliminary estimates of virtual velocity and sediment exchange rate derived from the two published data sets are broadly consistent with measurements from comparable fluvial systems. Collectively, these aims are intended to provide the first ingredients for a mechanistic theory of luminescence signal evolution in fluvial sand, and a first assessment of the potential use of such a theory for extracting information about sediment transport. Note that this study does not attempt to date the deposits but is instead using the sensitivity-corrected zero-age residual luminescence intensity, or zero age residual equivalent dose, as a proxy for sediment transport processes. In this paper, we use "luminescence" as shorthand for either the sensitivity-corrected luminescence intensity or equivalent dose following a one-to-one correlation between the two.

2. Model for Luminescence in Suspended Sand

Consider a channel control volume of width w, depth h, and stream-wise length Δx (Figure 1). The total energy stored by the trapped electron concentration of suspended sediment within the control volume, N_e, is described by a basic conservation equation:

$$\frac{\partial N_e}{\partial t} = Q_{\text{upstream}} - Q_{\text{downstream}} - Q_{\text{bleaching}} - Q_{\text{deposition}} + Q_{\text{entrainment}} \quad (1)$$

where the rate of change of total energy of trapped electrons $\partial N_e/\partial t$ (Joules per time) equals the sum of five energy fluxes of sediment (each with dimensions of Joules per time). These include influx by suspended-sand

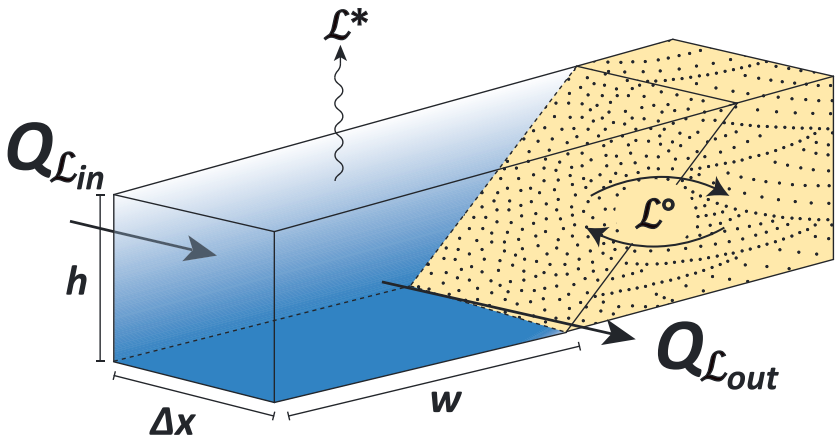

Figure 1. Definition diagram for the model used in this study. Luminescence equivalent dose, $\mathscr{L}$, is treated as a Eulerian quantity, whereby the transport of sediment by a river, the removal of luminescence by sunlight bleaching, and the erosion of new sediment are treated as conserved fluxes into and out of a control volume, Δxwh. $Q_{\mathscr{L}}$ is the flux of luminescence-bearing material, $\mathscr{L}^*$ is the luminescence lost to bleaching, and $\mathscr{L}^\circ$ is the influx of new luminescence due to erosion of new sediment with accumulated charge.

transport from upstream (Q_{upstream}), outflux by transport downstream ($Q_{\text{downstream}}$), loss of trapped electrons by sunlight bleaching ($Q_{\text{bleaching}}$), influx from entrainment of bed and bank sediment ($Q_{\text{entrainment}}$), and outflux by deposition ($Q_{\text{deposition}}$). The total energy within the control volume is

$$N_e = \Delta xwhC\mathscr{L}\rho \tag{2}$$

where C is the sediment volumetric concentration, ρ is the density of sediment, and $\mathscr{L}$ is the mean energy per kilogram expressed as equivalent dose (J/kg). Equivalent dose refers to the amount of absorbed radiative dose (J/kg) equivalent to produce the observed luminescence. The model is built around equivalent dose as this approach controls for downstream changes in luminescence sensitivity [*Murray and Wintle*, 2000; *Pietsch et al.*, 2008]. The model could also be built around sensitivity-corrected luminescence intensity where "sensitivity-corrected" means that the luminescence measurement is normalized by a small test dose of radiation such that luminescence measurements between different grains or aliquots are comparable. However, luminescence intensity is measured in arbitrary units and we use equivalent dose instead because this quantity has defined units (J/kg) which helps demonstrates the statement of conservation of energy used in the model. Here we define the *mean equivalent dose* as the arithmetic mean of all aliquots for a sample. We are interested in the average bulk behavior among all grains as no one grain of sand provides information about the transport histories of all grains. Using a mean value allows us to average the transport histories of many grains and obtain our desired information. The flux terms can be written as

$$Q_{\text{upstream}} = whuC\mathscr{L}(x)\rho \tag{3}$$

$$Q_{\text{downstream}} = whuC\mathscr{L}(x+\partial x)\rho \tag{4}$$

$$Q_{\text{bleaching}} = \Delta xwhC\mathscr{L}^*\rho \tag{5}$$

$$Q_{\text{deposition}} = \Delta xwhf_DC\mathscr{L}\rho \tag{6}$$

$$Q_{\text{entrainment}} = \Delta xwhf_EC\mathscr{L}_b\rho \tag{7}$$

where u is the "drift velocity" [*Pizzuto et al.*, 2016] of incoming sediment during transport, $\mathscr{L}^*$ is the rate of energy loss due to bleaching during transport (J/kg/s), f_D is the fraction of the suspended sediment load that goes into storage per second (s^{-1}), and f_E is the fraction of new suspended sediment entrained into the flow from storage (s^{-1}) with mean equivalent dose $\mathscr{L}_b$ (J/kg) (Figure 1). The drift velocity, u, is the time-averaged velocity of sediment during fluvial transport events. The variables, f_D and f_E, represent deposited or entrained volumes of sediment as a percent of the suspended load in the control volume. The volumetric flux of sediment q_s (m^3/s) is defined as

$$q_s = whuC \tag{8}$$

Multiplying both sides by u, treating u as constant in time and space, inserting equations (2) through (8) into equation (1), and dividing both sides by Δx, leads to the following equation:

$$\frac{\partial(q_s\mathscr{L})}{\partial t} = u\frac{q_s(x)\mathscr{L}(x)}{\Delta x} - u\frac{q_s(x+\partial x)\mathscr{L}(x+\partial x)}{\Delta x} - q_s\mathscr{L}^* - f_D q_s\mathscr{L} + f_E q_s\mathscr{L}_b \tag{9}$$

Taking the limit as Δx approaches zero, applying the definition of the derivative and expanding all derivatives by using the product rule leads to the complete equation:

$$q_s\frac{\partial\mathscr{L}}{\partial t} + \mathscr{L}\frac{\partial q_s}{\partial t} = -u\left[\mathscr{L}\frac{\partial q_s}{\partial x} + q_s\frac{\partial\mathscr{L}}{\partial x}\right] + q_s[f_E\mathscr{L}_b - f_D\mathscr{L} - \mathscr{L}^*] \tag{10}$$

Equation (10) describes conservation of energy stored as trapped electrons in the system with variable sediment transport rate (q_s) and sediment entrainment parameters (f_E, f_D). If equation (10) was applied to a stream reach with a steady and uniform suspended-sediment load, then the $\partial q_s/\partial x$ and $\partial q_s/\partial t$ derivatives would equal zero and q_s would cancel from all terms. If we further consider a channel reach in which deposition and entrainment rates are approximately in balance, then $f_E = f_D = \eta$, where η represents the sediment exchange rate (fraction of suspended sediment flux exchanged with storage centers per time). Under these conditions, the governing equation simplifies to

$$\frac{\partial\mathscr{L}}{\partial t} = -u\frac{\partial\mathscr{L}}{\partial x} - \mathscr{L}^* + \mathscr{L}^\circ \tag{11}$$

$$\mathscr{L}^\circ = \eta(\mathscr{L}_b - \mathscr{L}) \tag{12}$$

Equation (11) is a kinematic wave equation with source/sink terms that are controlled by the sediment exchange ($\mathscr{L}^o$) and bleaching efficiency ($\mathscr{L}^*$). The parameter $\mathscr{L}^*$ (J/kg/s) represents the effective bleaching rate of luminescence during transport. Its value depends on how fast a luminescence signal is removed, which depends on the duration and intensity of sunlight, modulated by latitude, time of day and year, atmospheric conditions (cloudiness), and river conditions (flow depth and water turbidity). The parameter $\mathscr{L}^\circ$ (J/kg/s) describes the effective flux of luminescence-bearing sediment into and out of active transport due to river erosion and deposition along the bed and banks. Luminescence measurements are typically made in the 90–250 μm grain size range, and therefore, this model is applicable to the transport of fine sand. We elaborate on these assumptions in section 4.

2.1. Definition of $\mathscr{L}^*$

To solve for the transport velocity (u), virtual velocity (U), and exchange rate (η) parameters, it is necessary to constrain the reduction rate of trapped-electron concentration due to sunlight exposure, $\mathscr{L}^*$. There are two conditions under which grains may be partially bleached: exposure to sunlight during subaqueous fluvial transport and illumination of a thin layer of surface during periods between high flows when the drop in the water level exposes sediment on the higher parts of bars and banks. We define $\mathscr{L}^*_{\text{fluvial}}$ as the rate of equivalent dose decrease due to bleaching during subaqueous fluvial transport and $\mathscr{L}^*_{\text{surface}}$ as the time-averaged rate of bleaching of a thin layer of deposited surface grains during low flows. The total rate of bleaching is then

$$\mathscr{L}^* = \mathscr{L}^*_{\text{fluvial}} + \mathscr{L}^*_{\text{surface}} \tag{13}$$

In this study, we assume that $\mathscr{L}^*_{\text{fluvial}}$ is significantly greater than $\mathscr{L}^*_{\text{surface}}$, because the latter involves only a small number of grains, and therefore, we only include the former term. This assumption may or may not be applicable to all river systems [e.g., *Porat et al.*, 2001] as some of the sediment entering the channel through entrainment might reasonably be expected to be material deposited during a recent event and exposed to sunlight during low-flow conditions. An example may be an ephemeral river where the riverbed is dry and exposed to sunlight for long periods. However, *McGuire and Rhodes* [2015b] noted that even the highly ephemeral Mojave River seems to demonstrate bleaching during transport rather than surface bleaching. We explore the consequences of this assumption further in section 4.

We take $\mathscr{L}^*_{\text{fluvial}}$ to be the derivative of equivalent dose with respect to time during sunlight exposure under fluvial conditions $\left(\frac{\partial D_E}{\partial t}\right)$. This derivative can be determined empirically from experiments in which aliquots of known dose are exposed to sunlight at various intervals [*McGuire and Rhodes*, 2015a]. These data should be fit

to an equation that can be differentiated to obtain $\left(\frac{\partial D_E}{\partial t}\right)$. We propose that the loss of equivalent dose due to bleaching could be described by a simple power law equation such as

$$D_E(t) = \left((\beta - 1)k_t t + D_0^{1-\beta}\right)^{\frac{1}{1-\beta}} \tag{14}$$

$$\mathscr{L}^*_{\text{fluvial}} = \frac{\partial D_E}{\partial t} = -k_t {D_E}^{\beta} = -k_t \mathscr{L}^{\beta} \tag{15}$$

where D_E is the equivalent dose (J/kg), β is a nondimensional constant, k_t is an effective loss rate for equivalent dose (s^{-1}), and D_0 is the initial equivalent dose (J/kg). Note that because we have formulated the model in terms of equivalent dose, D_E is the same as $\mathscr{L}$. Equations (14) and (15) offer flexibility in fitting the data from these bleaching experiments. If possible, it is best to perform these experiments under light conditions expected during floods, such as under turbid water. Some possibilities include laboratory experiment [*Ditlefsen*, 1992], flume study [*Gemmell*, 1985], or experimentation in a turbid field environment [*Sanderson et al.*, 2007]. Equations (14) and (15) are based on the assumption that the bulk bleaching rate of suspended grains in a well-mixed turbulent flow field has a similar power law function as direct sunlight bleaching, but with significantly lower bleaching rate parameters (k_t and β) than the direct-sunlight case. We show in the next paragraphs how we theoretically attenuate these bleaching rate parameters by using simple subaqueous light attenuation physics.

For the Mojave River data set, we use the bleaching experiment data of *McGuire and Rhodes* [2015a] to estimate $\mathscr{L}^*_{\text{fluvial}}$. Because they reported bleaching in terms of changes in luminescence intensity rather than equivalent dose, we need a method to translate between the two quantities. We use a saturating exponential of the form $y = A(1 - e^{-Bx})$, where A and B are constants, to express the relation between sensitivity-corrected integrated luminescence intensity I (arbitrary units) and the equivalent dose, D_E (J/kg). Using this approach, equivalent dose, D_E, can be derived from integrated luminescence intensity, I, as

$$D_E = -D_* \ln\left(1 - \frac{I}{I_{\text{sat}}}\right) \tag{16}$$

$$\frac{\partial D_E}{\partial t} = \frac{\partial I}{\partial t}\left(\frac{D_*}{I_{\text{sat}} - I}\right) \tag{17}$$

where D_* is a growth parameter (J/kg) and I_{sat} is the integrated luminescence intensity at saturation (arbitrary units). Note that sometimes the observed response of luminescence as a function of dose is better described with functions other than an exponential. The exponential function adequately describes luminescence growth for our purposes. We use a saturating exponential for simplicity and to capture the saturating nature of luminescence as a result of dose. This approach is also used for the Loire data set.

To define $I(t)$, we follow *McGuire and Rhodes* [2015a] and fit a power law to their data (similar to equation (14)), describing the change of luminescence intensity as a function of sunlight exposure time:

$$I(t) = \left((\beta - 1)ft + I_0^{1-\beta}\right)^{\frac{1}{1-\beta}} \tag{18}$$

where β represents the nondimensional decay order of the system, I_o is the initial integrated luminescence intensity and f describes the loss rate for integrated luminescence intensity (s^{-1}). Note that equation (18) describes the integrated luminescence photon counts versus sunlight exposure time for small aliquots. Equation (18) adequately fits their experimental data ($R^2 = 0.95$). To account for the effects of river turbidity, we consider that the loss rate f scales directly with light intensity integrated over the sunlight spectrum:

$$f = \int \varphi(\lambda)\gamma(\lambda)\partial\lambda \tag{19}$$

where $\varphi(\lambda)$ is the incoming photon flux (sunlight) for a given wavelength λ (photons/cm^2/nm) and $\gamma(\lambda)$ is the scaling of the loss rate f with photon flux under a given wavelength (cm^2/photons). Note that $\gamma(\lambda)$ is not strictly a photoionization cross section but rather a value describing the change in loss rate of integrated luminescence intensity or equivalent dose due to variable sunlight intensity.

The incoming photon flux, $\varphi(\lambda)$, can be described to a first approximation by the Beer-Lambert law in photon-flux form for the attenuation of light in a fluid medium:

$$\varphi(\lambda) = \varphi_o(\lambda) e^{-\frac{z_{\text{eff}}}{z_*(\lambda)}} \tag{20}$$

The variable $z_*(\lambda)$ represents the attenuation of sunlight per wavelength in turbid water. The variable z_{eff} represents the effective depth in the fluid at which a grain isolated at that depth would receive the same total amount of light as that expected for a grain undergoing random, turbulence-driven motion throughout the water column (see the supporting information for its derivation). We simplify equations (19) and (20) by assuming no wavelength dependence on the loss rate. With this simplification, $f = \gamma\varphi$ and the unattenuated loss rate $f_o = \gamma\varphi_o$ such that

$$f = f_o e^{-\frac{z_{\text{eff}}}{z_*}} \tag{21}$$

which is then inserted into equation (18). Equation (21) assumes that the magnitude of light intensity with depth exerts a stronger control on the loss rate than attenuation due to spectral filtering by absorption of some wavelengths of light by water. The filtering of higher-energy wavelengths of light can lower bleaching rates [*Sanderson et al.*, 2007; *Kars et al.*, 2014], but because we consider that fluid turbulence moves grains toward the surface of the flow, where spectral filtering is minimal, this is less important than the overall light intensity in water. We explore this assumption further in section 4, but note again that this assumption can be avoided by performing experiments to fit equations (14) and (15).

2.2. Definition of the Storage Center Sediment Dose $\mathscr{L}_b$

In order to implement the model, it is necessary to establish the luminescence input from entrainment of sediment, $\mathscr{L}_b$. We propose that this value can (a) be determined empirically through measurements of sedimentary deposits near the river, (b) be calculated from the sediment residence time distribution and background dose rate, (c) or can be calculated with a process-based sediment transport model. For this study, we follow the first approach (a) and treat luminescence data from deposits near the river as $\mathscr{L}_b$ and use this value to calculate the characteristic storage time scale, τ_s. To do this, the mean equivalent dose of sediment that appears to be on the verge of erosion, such as the outer banks of meander bends, is taken as $\mathscr{L}_b$ and divided by the average dose rate of the storage center, D_R (J/kg/kyr), to solve for τ_s (e.g., the relationship in equation (22)). Ideally, this empirical approach should involve a large number of samples to ensure accurate estimation of $\mathscr{L}_b$. This approach has the benefit of robustly determining $\mathscr{L}_b$ and can also examine its spatial distribution.

If the distribution of sediment residence time was known, the equivalent dose of basal sediment $\mathscr{L}_b$ could be taken as an expected value of sediment residence time τ_s multiplied by the background dose rate as a function of space and/or time $D_R(x, t)$:

$$\mathscr{L}_b = D_R(x,t)\cdot\tau_s \tag{22}$$

$$\tau_s = \int_0^\infty t_s p(t_s) dt_s \tag{23}$$

where t_s is time spent in storage and $p(t_s)$ is the probability density function of sediment storage time. Note that this formulation assumes that the characteristic time scale of storage is below the saturation limit for the luminescence signal of interest. If the model is formulated in terms of luminescence intensity, then equation (22) can be converted by using equation (17). The expected value (similar to the weighted mean) in equation (23) depends on the probability density function $p(t_s)$ chosen to represent the system of interest. Determining $p(t_s)$ is beyond the scope of this paper, though significant research exists on this topic [e.g., *Bradley and Tucker*, 2013, and references therein]. In the simplest case, $p(t_s)$ could be assumed as an exponential distribution constrained by field measurements. However, it is noted that this may not be appropriate for all systems. In some cases, the integral described in equation (23) may not have a finite expected value if $p(t_s)$ is governed by heavy-tailed probability distributions [*Bradley and Tucker*, 2013].

Finally, an alternative method to evaluate $\mathscr{L}_b$ would be to use a landscape evolution model constrained by field data. One example could be a meandering river system coupled with sediment transport modeling [*Bradley and Tucker*, 2013]. For illustrative purposes, we consider a simple system where a channel can access all of the storage center with equal probability. In this case, the rate of change in basal equivalent dose with time is

$$\frac{\partial \mathscr{L}_b(x)}{\partial t} = D_R + \eta f_V(\mathscr{L}(x) - \mathscr{L}_b(x)) \tag{24}$$

where f_V is the ratio between the sediment volume in the channel and volume in the storage center. Combining equation (24) with the transport, equations (11) and (12) produce a simple system where equivalent doses decrease during transport and increase during storage.

2.3. Estimation of Time-Averaged Virtual Velocity *U*

In this section, we consider how time-averaged virtual velocity, defined as the velocity of sediment grains that alternate between periods of mobility and periods of storage [*Martin and Church*, 2004], relates to other parameters in the model. Virtual velocity may be quantified as

$$U = \frac{\text{total distance of travel}}{\text{total time in transport} \;+\; \text{total time in storage}} \tag{25}$$

At any given moment, the vast majority of grains will normally reside in a storage center [*Meade*, 2007]. When storage time ≫ transport time, the ratio between the characteristic lengthscale sediment travels before deposition (ℓ_s) and the characteristic time scale of sediment storage (τ_s) provides an approximation of the time-averaged virtual velocity [*Martin and Church*, 2004; *Pizzuto et al.*, 2014]:

$$U \cong \frac{\ell_s}{\tau_s} \tag{26}$$

Pizzuto et al. [2014] and *Lauer and Parker* [2008b] give relations for the characteristic transport lengthscale (ℓ_s) which we modify slightly to produce the correct units from our model-derived values:

$$\ell_s = \frac{up_c}{\eta\, p_f} \tag{27}$$

where p_c and p_f are the relative concentrations of sand and silt grain sizes in the river channel sediment, here taken as equal for simplicity. The characteristic lengthscale is the downstream distance over which 1/e (~37%) of the suspended sediment volume enters storage [*Lauer and Willenbring*, 2010; *Pizzuto et al.*, 2014]. Combining equations (26) and (27),

$$U = \frac{u/\eta}{\tau_s} \tag{28}$$

This relation indicates that if sediment drift velocity, exchange rate, and storage residence time were known, then one could also obtain virtual velocity.

3. Results

3.1. Model Behavior and Predictions

The model presented above demonstrates a series of behaviors and makes several predictions about the magnitude and spatial pattern of equivalent dose in river channel fine sand (Figure 2). Consider the case of a channel reach with uniform discharge, in which suspended sediment enters at the upstream end at a steady rate and with a constant initial luminescence signal. In this case, the model predicts that the equivalent dose in river channel sediment will tend to approach a steady value over some length scale; in other words, once suspended sediment has traveled beyond a certain distance downstream of the head of the reach, its mean equivalent dose becomes approximately uniform ($\partial L/\partial x \approx 0$). At this point, the suspended sediment has reached a state of equilibrium in which the influx of fine sand with high equivalent dose from storage centers is matched by the decrease due to sunlight bleaching. This is a theoretical state that a river would reach under constant forcing, that is, approximately constant sediment flux and approximately unchanging sediment transport parameters, u and η, and if the sediment in the channel and storage center is well mixed with regard to equivalent dose. A change in the bleaching rate (L^*) or the equivalent dose of sediment eroded from storage ($\mathscr{L}_b$) will change the steady value. For example, a lower bleaching rate (L^*), such as one might find by measuring a slow to bleach luminescence signal, implies a higher steady value than would a higher bleaching rate associated with fast-to-bleach signals (Figure 2). An increase in the background luminescence ($\mathscr{L}_b$), due, for example, to erosion of an older fill terrace with higher dose, would be associated with an increase in the mean equivalent dose of in-channel sediment (Figure 2). Spatial perturbations to this steady value cause either an increase or decrease before returning to the steady value. For example, a tributary that introduces relatively unbleached sediment with higher dose would cause a "spike" in the river channel mean equivalent dose, which eventually returns to the steady value farther downstream (Figure 2). Similarly, entrainment of sediment with near-zero equivalent dose along a particular reach of the channel would cause a transient decrease in river channel mean equivalent dose for some distance downstream.

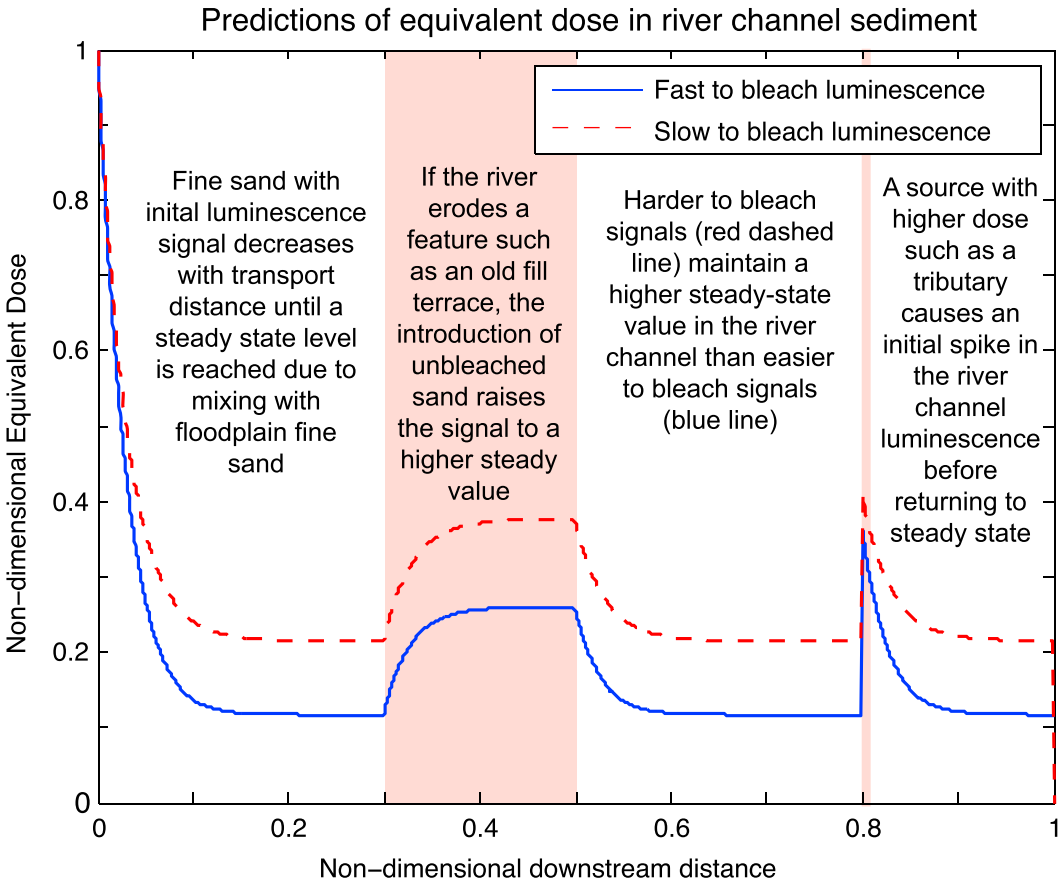

Figure 2. Predictions of the downstream patterns in luminescence equivalent dose of river sediment represented by Figure 1 and equation (10). The blue line represents the model by using a fast to bleach luminescence; the dashed red line shows a slower-to-bleach luminescence.

It is important to note that the model does not necessarily predict that luminescence starts at a high value and decreases downstream, but rather that the starting luminescence, whether bleached or unbleached, will increase or decrease until it reaches a steady value, which reflects a balance between loss of luminescence due to bleaching and influx of sediment from storage centers where regeneration can occur. The model solutions shown in Figure 2 treat the stored-sediment luminescence, $\mathscr{L}_b$, as a boundary condition. What happens when the luminescence is allowed to evolve dynamically, as described by equation (24)? To address this question, we couple equation (24) with equations (11) and (12) to produce a simple system wherein an initial influx of sediment with some equivalent dose enters from upstream and subsequently undergoes either transport, where it is bleached, or enters into storage where it is able to regenerate at some background dose rate (Figure 3). Both fast-to-bleach luminescence and slow-to-bleach luminescence (such as quartz OSL versus pIRIR_{290}) show similar patterns; the upstream reaches display either an increase or decrease in equivalent dose with transport distance until a steady state condition is reached, downstream of which the equivalent dose is constant with distance. In this simple theoretical example, the mean equivalent dose in the storage center is higher than the mean equivalent dose in the channel for both signals. As in Figure 2, any changes due to additional sediment transport processes may change the steady state value and introduce some downstream variation. However, the essence of the prediction, for both in-channel and floodplain sediment, is a gradual downstream decrease or increase in luminescence that asymptotes to a quasi-uniform value. For suspended sediment in the channel, this uniform value represents a balance between the addition of signal via entrainment of stored sediment, and the loss of signal to bleaching. For stored sediment, the predicted emergence of constant average luminescence downstream reflects a balance between signal acquisition from ionizing radiation, and signal loss due to dynamic sediment exchange with the channel.

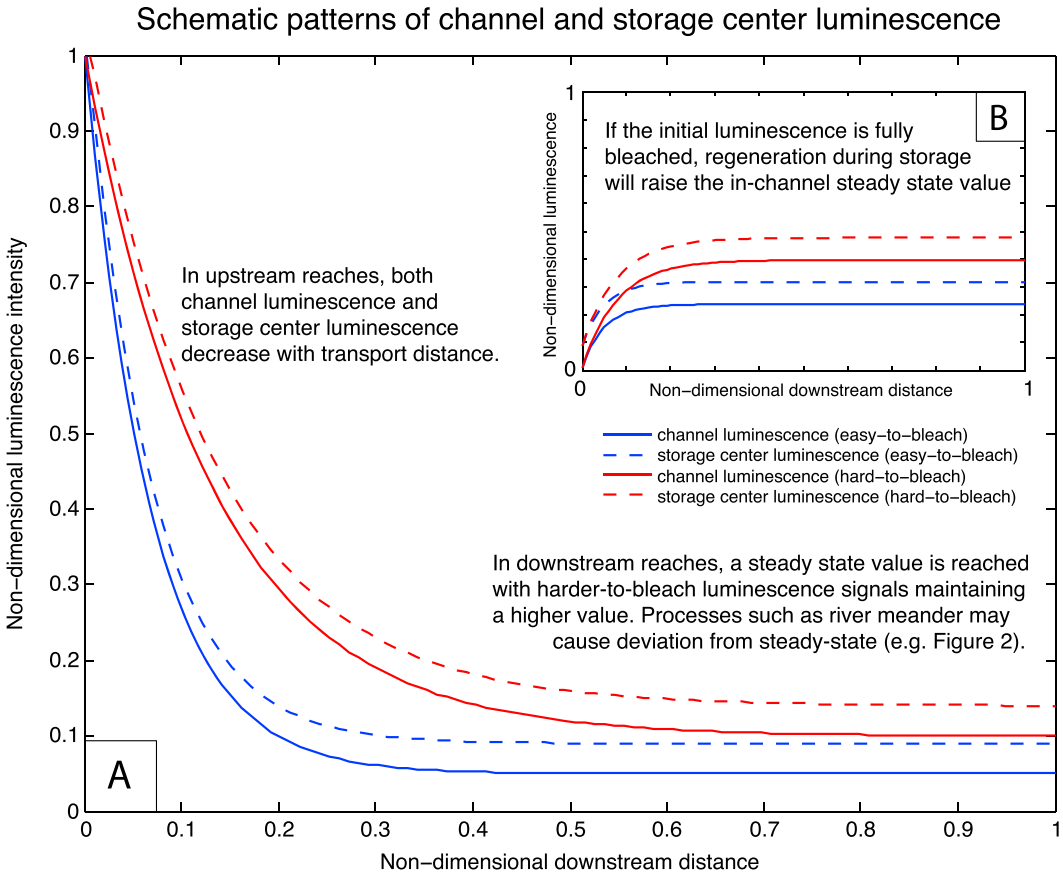

Figure 3. (a) Example of a simple storage center interaction with channel sediment. Storage center is modeled with equation (24), and transport is modeled with equations (11) and (12). (b) Example of a system where the initial sediment is fully bleached. Regeneration during storage causes the in-channel luminescence to increase until steady state is obtained.

3.2. Comparison With Field Data

As a test of the model predictions, we compared the model with previously published measurements of luminescence/equivalent dose in river sediment for two very different river systems, the Mojave River in southern California, USA [*McGuire and Rhodes*, 2015a] (Figure 4), and the Loire in France [*Stokes et al.*, 2001] (Figure 5). The Mojave River is a regional-scale (~10^2 km long), single-channel, desert ephemeral river which undergoes a large flood once every ~10 years [*McGuire and Rhodes*, 2015b]. In contrast, the Loire is a continental-scale (~10^3 km long), meandering, temperate-climate, perennial river that undergoes yearly flooding [*Stokes et al.*, 2001]. Despite dissimilar hydrology, both data sets show an overall decrease in the measured luminescence with downstream distance (for feldspar MET-pIRIR$_{230}$ for the Mojave and quartz OSL in the Loire), albeit with some notable deviations (Figures 4 and 5). In both data sets, the steady value at $\partial L/\partial x \approx 0$ is greater than would be expected for a fully bleached sample. In the Mojave River data set, the signals measured from the river sediment are much greater than what is observed from a fully sunlight-bleached sample [*McGuire and Rhodes*, 2015a]. In the Loire, channel equivalent doses at the downstream reaches demonstrate large variability, but some data points are significantly lower than samples in the upstream reaches as discussed below.

In the Mojave River data set, *McGuire and Rhodes* [2015a] collected samples from 0.3 to 0.5 m depth in dry channel bar deposits with developed bedding structures. Equivalent dose for each sample was measured by using the MET-pIRIR protocol [*Li and Li*, 2011] with post-IR temperatures of 95, 140, 185, and 180°C. The equivalent dose can be seen to follow a generally downstream-decreasing pattern with increasing transport distance (Figure 4). However, the downstream-most sample departs from this trend. Its location correlates with a downstream change in channel morphology from a relatively wide channel to a narrow reach with considerably higher and steeper valley walls [*McGuire and Rhodes*, 2015a, 2015b]. We interpret the data in Figure 4 as indicating that the upstream reaches of the Mojave follow a pattern of equivalent doses

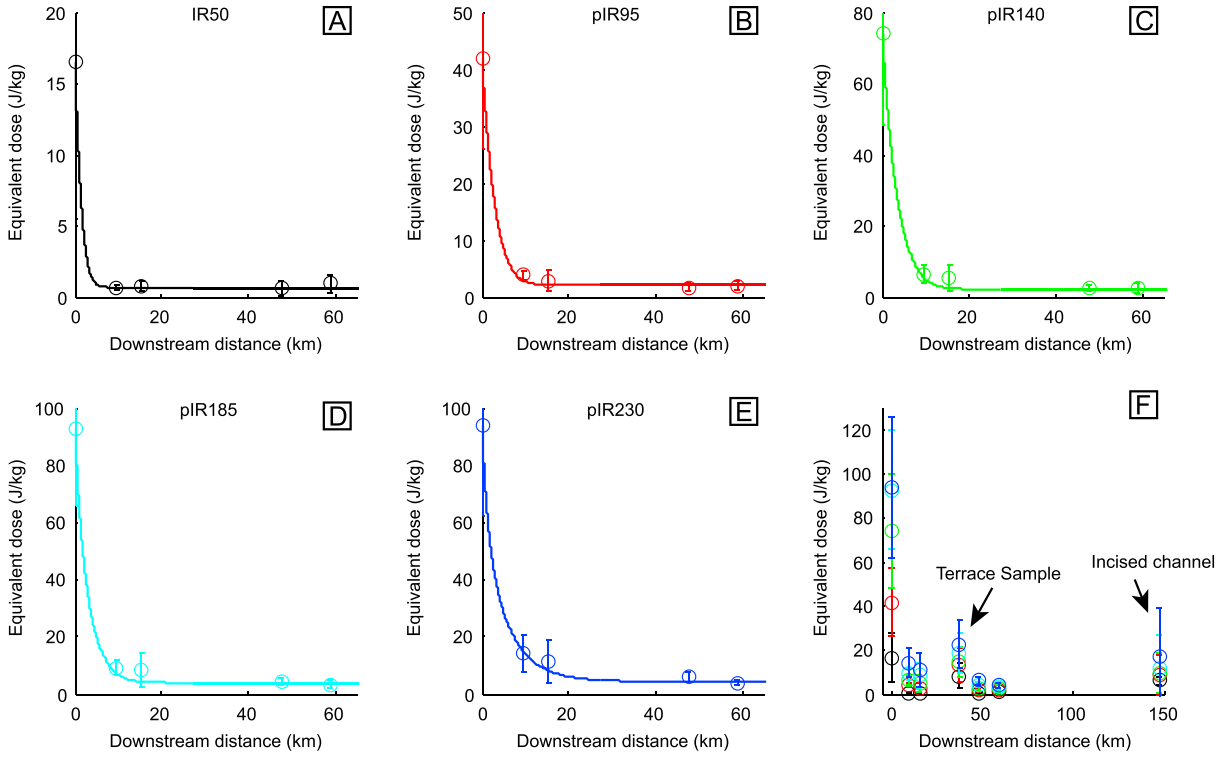

Figure 4. Application of the model to field data from *McGuire and Rhodes* [2015a] for the Mojave River in Southern California, USA. (a–e) Comparison of field data (circles with error bars) with best fitting model run (line) for various pIR signals. (f) Complete field data from McGuire and Rhodes data including terrace sample used for storage center luminescence and incised channel sample not included in study due to strong change in river geomorphology.

declining downstream toward a steady value, whereas the downstream incised reaches demonstrate a potential increase in the equivalent dose of basal sediment $\mathscr{L}_b$ and/or represent a change in relative magnitude between the erosional exchange f_E and depositional exchange f_D. Because the exact roles of either cause are not constrained, we treat the farthest downstream sample as an outlier and exclude it from the model. If information such as the $\mathscr{L}_b$ value in the downstream reaches were known, then it would allow the modeling of this part of the system. However, the model presented here provides a consistent explanation for these observations (Figure 2).

For the Mojave River case, the loss rate f and decay order β (equation (18)) were directly measured through the bleaching experiments of *McGuire and Rhodes* [2015a]. We use the dose recovery data, in the form of parameters relating equivalent dose to sensitivity-corrected luminescence intensity, D_*, and I_{sat}, from *McGuire and Rhodes* [2015a] for equations (16) and (17). The river during major transport events was taken to be turbid: z_* was assumed to be 5 cm and constant across the sunlight spectrum. We estimated z_* by observing a video of the Mojave River during a major flood and estimating the depth to which submerged objects became obscured. We then converted this depth to a light attenuation constant by using an empirical relation for desert lakes [*Idso and Gilbert*, 1974]. This is a reasonable approximation considering the complexity of river turbidity [*Belmont et al.*, 2009] and the fact that no theoretical relation exists for river turbidity [*Davies-Colley and Smith*, 2001] although empirical relations for select rivers exist [*Davies-Colley and Nagels*, 2008; *Julian et al.*, 2008]. We assume that the in-channel sediment has undergone turbulent transport in these turbid conditions prior to deposition in channel bars from which our two data sets were sampled [*Stokes et al.*, 2001; *McGuire and Rhodes*, 2015a]. The $\mathscr{L}_b$ value was determined from a terrace sample from *McGuire and Rhodes* [2015a] (Figure 4).

We applied the model to the Mojave River by running the model under the parameters described above. Only in-channel samples, including channel bars, were used to model the channel sediment luminescence. The terrace data were used to calculate the channel/storage center exchange ($\mathscr{L}^*$). The model was run repeatedly, and the parameters of u and η were systematically changed on each iteration to find the best fit ting run as determined by least squares regression (see the supporting information). After the best fit values for u (transport velocity) and η

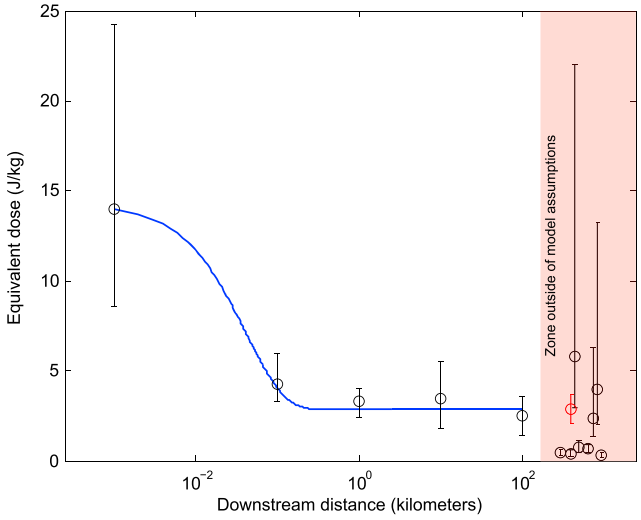

Figure 5. Application of the model to quartz OSL field data [*Stokes et al.*, 2001] for the Loire in France. Note the logarithmic scale used for *x* axis following original presentation of data in *Stokes et al.* [2001] and to better illustrate model/data comparison. Apparent convexity in the curve is a result of logarithmic *x* axis scale. Errors on data points taken as half of the maximum and minimum reported values from *Stokes et al.* [2001]. Farthest downstream samples are not modeled due to uncertainties in sediment flux, storage times, and consistency of exchange rates. See text for discussion. The red circle indicates terrace data from *Colls et al.* [2001] used to calculate example storage time scales and exchange rates.

(sediment exchange rate) were obtained, we used those values, and the terrace sample of *McGuire and Rhodes* [2015a], to obtain $\mathscr{L}_b$ and to calculate the characteristic transport lengthscale, ℓ_s; characteristic storage time scale, τ_s; and time-averaged virtual velocity, *U*. The model was run for each set of MET-pIRIR luminescence signals, which produced transport values that were internally consistent and within uncertainty. The values were then averaged and are reported in Table 1. Application of the model to the Mojave River results in a sediment exchange rate for fine sand of 17% ± 12% suspended load exchanged per kilometer, characteristic transport lengthscale of 6.9 ± 4.2 km, characteristic storage time scale of 3.6 ± 1.2 kyr, and time-averaged virtual velocity *U* of 1.9 ± 1.4 km/yr (Table 1). These values are applicable to fine sand (90–250 μm).

The Loire data set was obtained from *Stokes et al.* [2001], who collected samples by placing empty cans with a volume of ~333 cm^3 into unconsolidated sediment below 60 cm of water and immediately transferring the can to a light-proof polyethylene bag. Samples were collected at logarithmic spacing for the first 100 km and then at approximately 100 km increments further downstream [*Stokes et al.*, 2001]. They used a single aliquot regeneration protocol with a single regeneration point of 4 J/kg and a linear fit to the resulting growth curve. The measured equivalent dose shows a general decrease in equivalent dose with downstream distance similar to the Mojave River data set (Figure 5). However, this pattern breaks in a location that roughly correlates with a shift from rural to urban land use as well as junctions with six large tributaries [*Stokes et al.*, 2001]. We do not apply the model to the full system of the Loire because of the assumptions used to derive the simplified model. These assumptions are approximately constant sediment load, constant bleaching rate, and approximately constant $\mathscr{L}_b$. Instead, we apply the model to the upper reaches of the Loire where we are more confident that our assumptions are valid.

For the case of the Loire, data to calculate k_t and β are not available. For illustration, we model the bleaching of luminescence intensity and convert it to equivalent dose so that this data set can be used to estimate sediment transport information. We estimate *f* by using the blackbody irradiation of the Sun filtered through atmospheric and subaqueous conditions and the photoionization cross section of quartz OSL [*Singarayer and Bailey*, 2004; *Bailey et al.*, 2011], and the decay order, β, is taken as 1. This is not strictly correct as γ in equation (18) is not the same as the photoionization cross sections of quartz [i.e., *Jain et al.*, 2003], and the measurement of quartz OSL in the Loire involved a combination of multiple quartz OSL components leading to a different β [*Bailey et al.*, 1997]. Further detail is provided in the supporting information. The *e*-folding length z_* was taken to be 5 cm and constant across the sunlight spectrum for both rivers. We used the modern and T1 terrace data from *Colls et al.* [2001] to estimate $\mathscr{L}_b$. Because no data on the dose-response curves for the Loire are available, we used data from the recent laboratory intercomparison quartz standard [*Murray et al.*, 2015] to estimate D_* and I_{sat}.

We applied the model to the Loire following the same order of operations as the application of the model to the Mojave River, using the parameters above to find the best fit values of *u* (transport velocity), and η (sediment exchange rate). Application of the model results in a sediment exchange rate (η) for fine sand of

Table 1. Values Obtained From Application of the Model to the Field Data of *McGuire and Rhodes* [2015a] for the Mojave River and the Field Data of *Stokes et al.* [2001] and *Colls et al.* [2001] for the Loire[a]

River	Luminescence Signal	Sediment Exchange Rate η	Transport Lengthscale ls (km)	Long-Term Storage Time Scale τ_s (kyr)	Time-Averaged Virtual Velocity U (m/yr)
Mojave River, USA	pIR230	11% ± 6% per km	8.7 ± 4.5	5.2 ± 1.5	1.7 ± 1.0
	pIR185	20% ± 10% per km	10 ± 5.1	4.2 ± 1.3	2.4 ± 1.4
	pIR140	17% ± 11% per km	7.7 ± 4.7	3.6 ± 1.0	2.1 ± 1.4
	pIR95	19% ± 7% per km	4.8 ± 1.8	3.3 ± 1.1	1.5 ± 0.7
	IR50	18% per km	3.6	2.1 ± 0.9	1.7
	Average value	*17% ± 12% per km*	*6.9 ± 4.2*	*3.6 ± 1.2*	*1.9 ± 1.4*
Loire River, France	Quartz OSL	4.7% ± 4.2% per m	0.05	1.2 ± 0.75	0.04
Ranges observed in previously published data	Nonluminescence methods	1.6%–44% per km	0.4–113	0.125–1.8	0.8–200

[a]Ranges from previously published data from *Pizzuto et al.* [2014] are given in the bottom row for comparison. Storage time scale range is based on mean post-settlement age to mean presettlement age. Uncertainties are reported to 1σ. Values with no uncertainty have relative errors greater than 1 and are shown for illustrative purposes. The sediment exchange rate η is converted from units of (s^{-1}) to (m^{-1}) or (km^{-1}) by dividing η by the transport velocity u and converting to meters or kilometers for direct comparison to the characteristic transport distance commonly used in sediment-budget studies [e.g., *Pizzuto et al.*, 2014]. The exchange rate, η, for the Loire is given in units of % per meter as the rate in units of % per kilometer is over 100%.

4.7% ± 4.2% fraction suspended load exchanged per meter, characteristic transport lengthscale of 50 m, characteristic storage time scale of 1.2 ± 0.75 kyr, and time-averaged virtual velocity, U, of 0.04 km/yr (Table 1). Transport velocity u, sediment-exchange rate η, and associated uncertainties were determined by least squares fitting (see the supporting information). These values are applicable to fine sand (90–250 μm). The large uncertainties in the Loire data set lead to large uncertainties in the model fits. For the transport lengthscale, storage time scale, and virtual velocity, the relative uncertainty is over 100%, and as such we show the resultant values simply for illustration. Note that in the application to both the Mojave and Loire, we are using single-aliquot data. It may be preferable to use large aliquots in order to capture the histories of many grains to describe the bulk behavior of all grains.

A simplified sensitivity analysis of how changes in the best fit values of u and η for the Loire and the Mojave is given in Figure 6. In our analysis, we held the best fit u or η constant and varied the other parameter. Both model runs are sensitive to changes in u and η. Percent changes on the order of around 50–100% are sufficient to cause a significant deviation from the best fitting model run. For the Mojave river, a change in u leads to a significant misfit of the model to the samples taken at approximately 10 and 15 km downstream. However, the model fit to the downstream samples at ~48 and ~59 km are largely unaffected by changes in u. In contrast, the converse is true for changes in η where the downstream samples are easily misfit with changes in η, whereas the fit for the upstream samples are unaffected. For the Loire, a similar effect can be observed. However, the model run for the Loire is largely insensitive to changes in the exchange rate in the downstream reaches. This is a consequence of this particular data set as the exchange rate is already very high due to the luminescence value used from the *Colls et al.* [2001] data set. Note that in both the 0–10 km reaches of Figure 6b and the reach downstream of 0.1 km in Figure 6d, the exchange rate shifts the curve in an opposite manner than it does in the downstream reaches. The location where this behavior shifts, at ~12 km in Figure 6b and ~0.7 km in Figure 6d, indicates a change from an advection dominated system to a system dominated by the exchange rate.

4. Discussion

4.1. Model Application to the Mojave and Loire

To our knowledge, this is the first mechanistic model based on conservation of mass and energy that provides an explanation of the spatial patterns of luminescence in river channel sediment. The best fit sediment transport parameters from application of the model span a broader range of values than those reported in the literature. However, the results are nonetheless encouraging in terms of deriving information about fine-sand sediment transport from luminescence measurements (Table 1).

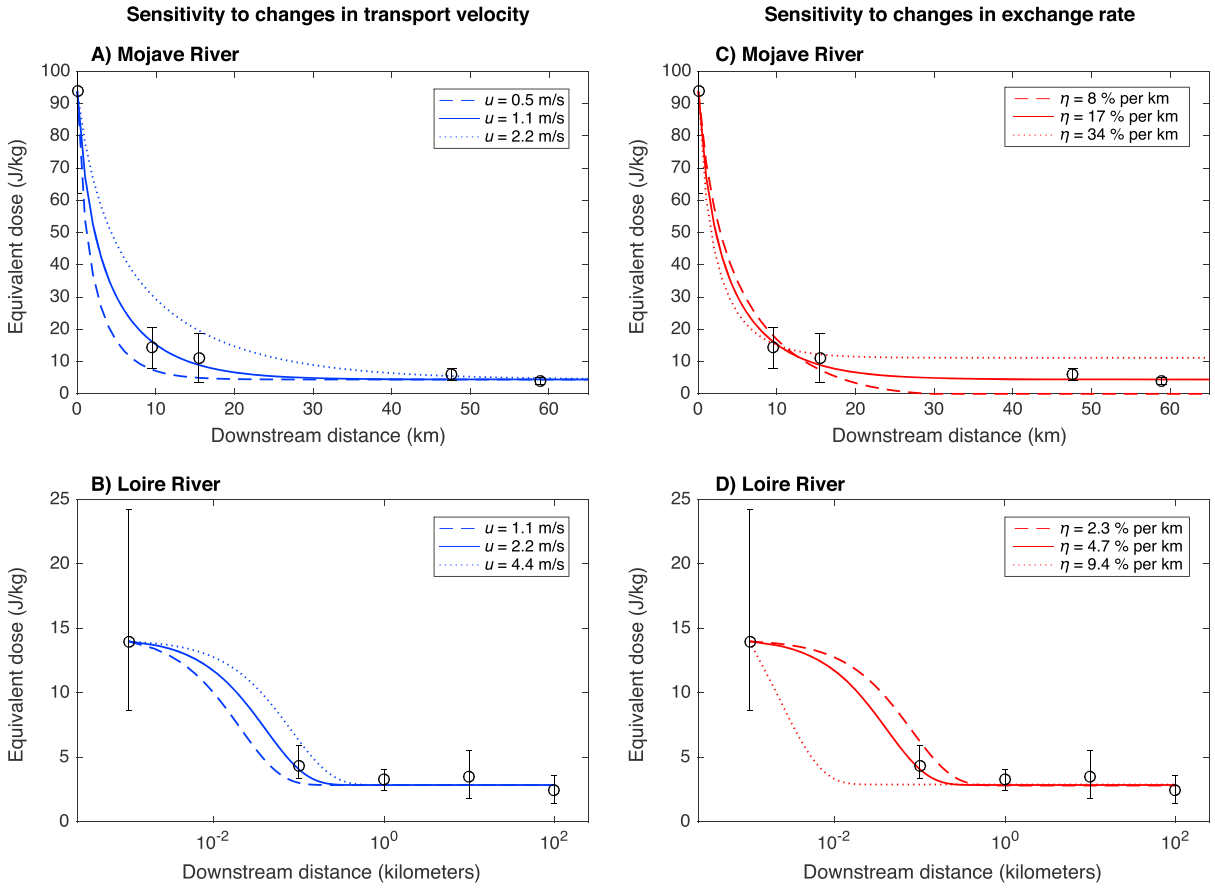

Figure 6. Example sensitivity analysis of the model application to the pIR230 data set from the Mojave River and to the Loire quartz OSL data set. (a and b) Example of how changes in the value of the transport velocity, u, affect the model. The solid blue line shows the best fit u value from Figure 4. The dashed line and dotted lines show the model changes when the u value is halved or doubled, respectively. (c and d) Example of how changes in the value of exchange rate, η, reflect in the model. The solid blue line shows the best fit η value from Figure 4. The dashed line and dotted lines show the model changes when the η value is halved or doubled, respectively. The best fit u and η apparently form a unique solution when fitted to the field data for the Mojave but not the Loire. This is because the data used to estimate the storage center luminescence are similar in equivalent dose to the channel luminescence, meaning that the η value is a minimum value.

Evaluating the accuracy of the method is complicated by the lack of data on exchange rates, characteristic length and time scales, and virtual velocities for fine sand [*Parsons et al.*, 2015]. Virtual velocity has largely been used to describe the movement of pebble and cobble tracers that travel as bed load [*Hassan et al.*, 1992; *Haschenburger and Church*, 1998; *Bradley and Tucker*, 2012]. However, recent work also uses the virtual velocity concept to understand long-term suspended sediment transport [*Pizzuto et al.*, 2014; *Parsons et al.*, 2015], particularly because of the tendency for contaminants to sorb onto fine sediment [e.g., *Pizzuto et al*, 2014]. *Pizzuto et al.* [2014] present the largest compilation to date ($n = 5$) of the exchange rates, characteristic length and time scales, and virtual velocities for fine sand resulting from a small number ofstudies in the Mid-Atlantic region of the northeastern United States by using nonluminescence methods. Their range in values is compared to our results in Table 1.

Our results show a broader range than observed in the *Pizzuto et al.* [2014] study. The values derived from the Mojave River data set are concordant with the order of magnitude ranges except for the storage time scale. The values derived from the upper Loire data set are outside the ranges, except for the storage time scale, and seem to present values representing a system with much slower sediment transport than seen in the *Pizzuto et al.* [2014] data. The apparent match between some of the Mojave River results with the previously published data is encouraging, particularly because of the inclusion of bleaching experiment data which were not available for the Loire data set. However, the results from the Loire data set may be anomalous. Our values are notably outside of the ranges in the *Pizzuto et al.* [2014] data set. The characteristic transport lengthscale of about 50 m seems short for suspended sediment transport. There may be two reasons for the

apparently anomalous results. The first possibility is that because we are unable to perform bleaching experiments on the Loire quartz, and have to use a theoretical value, we are using an incorrect bleaching rate. An incorrect bleaching rate could cause anomalous results in our best fit transport velocity and exchange rate. The second possibility is that quartz OSL may bleach too fast to be an effective tracing tool. As discussed later, a breakdown in scaling between the amount of bleaching and transport distance may occur when grains become fully bleached. If a grain fully bleaches within 50 m, then even if it travels further, this information is not tracked by the luminescence. This breakdown would violate our assumption that each grain records the full distance of its transport episode.

Alternatively, the Loire may be an anomalous river with very rapid sediment exchange. There are observations that show that rivers with smaller drainage area are associated with higher exchange rates [*Pizzuto et al.*, 2016]. The headwaters of the Loire may fit this interpretation although the results are still very low compared to compilations [*Pizzuto et al.*, 2014, 2016]. *Pizzuto et al.* [2014] note that the expected true range of characteristic scales, virtual velocities, and exchange rates may span orders of magnitudes beyond what they observe. They note that a continuum of transport length and time scales exists for shorter-term transport observed from tracer experiments and organic matter and that it is reasonable to suggest that a continuum exists for longer transport scales. Furthermore, the rivers from the northeastern United States explored by *Pizzuto et al.* [2014] have notably different morphologies than either of our literature-derived data sets. The *Pizzuto et al.* [2014] data set shows a large range over orders of magnitude for a small number of rivers ($n = 5$). Our results that lie partially outside the ranges previously observed are not necessarily unexpected and indicate that further research on the natural variability of these values is warranted. A more rigorous evaluation of our approach would require paired luminescence and sediment transport measurements at the same field site.

The applicability of the simplified model (equations (11) and (12)) depends on a series of assumptions. These assumptions indicate (1) that the majority of bleaching of trapped charge occurs during fluvial transport, (2) that characteristic transport and storage lengthscales and time scales for a river system have finite averages and/or variance, (3) that steady state approximations are appropriate over suspended sediment transport time scales, and (4) that no significant geomorphic disequilibria such as major changes in sediment supply are occurring over the time scales of fine sediment transport. We discuss these topics below.

4.2. Bleaching During Transport

Two central assumptions on the bleaching of luminescence were used in this model. First, we assume that removal of trapped charge largely occurs during in-channel transport by water. The counterpoint to this assumption is the possibility that the majority of bleaching occurs while sand is exposed at the surface of depositional units [*Porat et al.*, 2001; *Gray and Mahan*, 2015]. The relative role of surface bleaching versus transport depends on the size of the river system, the magnitude/frequency of transport, the turbidity of the water, and the effective depth to which sunlight can penetrate stationary sediment.

The relative volumes of surface-bleached material versus in-transport bleaching depend on the relative scaling of bleaching depth versus scour depth. Investigating luminescence as a surface exposure chronometer, *Sohbati et al.* [2012] found that the depth to which sunlight penetrates and bleaches Navajo Sandstone is on the order of 2–4 mm for ~80 years of sunlight exposure and 4–8 mm for 713 ± 61 years [*Sohbati et al.*, 2012]. For granite, *Sohbati et al.* [2012] modeled bleaching at approximately 12.5–17.5 mm depth for 10^2 years and approximately 15–20 mm depth for 10^3 years. Whether the bleaching depths of unconsolidated sediment follow this pattern is not yet known but may be on the same order of magnitude. Surface exposed sediment may also be bioturbated to deeper depths although the rate and magnitude of this depend on local biota. We estimate that bleaching in sediment reaches depths of 1–20 mm for the limited time sediment is in temporary in-channel storage such as bars. The expected depth to which sediment will be scoured and mobilized is a fractional power function of discharge, which depends on grain size and local river geometry [*Leopold et al.*, 1966; *Lu et al.*, 2012]. Bleaching depths are likely small compared to typical scour depths [*Leopold et al.*, 1966], causing small or annual floods to largely rework surface bleached sediment. Scour depths for large floods in midsized rivers similar to those in this study can be on the order of 0.5 to 1–2 m. If the depth expected to have been bleached by surface exposure is on the order of a few percent of the scour depth for characteristic "effective discharge" floods [*Wolman and Miller*, 1960], then it could be assumed that the transport bleaching is dominant. This is further supported by the observation that smaller yearly floods move negligible volumes of sediment when compared to the larger characteristic floods that move the majority of sediment [*Nash*, 1994].

If significant, the effect of the surface bleaching could potentially cause an underestimation of the modeled transport velocity and an overestimation of the sediment exchange rate due to more efficient bleaching than expected. In this case, a value for $\mathscr{L}^*_{surface}$ is needed to reflect entrainment of this bleached sediment. However, the best method to obtain this value is not immediately clear.

The second assumption used in this model is that while fine sand is in suspended transport, the role of spectral attenuation by water is less important than the magnitude of sunlight intensity. Evidence for a dependence of bleaching rate on wavelength has been previously explored and shown to have a notable effect [*Singarayer and Bailey*, 2004; *Sanderson et al.*, 2007; *Kars et al.*, 2014]. However, *Ditlefsen* [1992] noted that clear water played little role in the bleaching of potassium-feldspar OSL and thermoluminescence compared to sunlamp exposure. The role of wavelength dependence in this model is complicated by the rapid turbulent mixing of fine sand in suspension. The grain sizes commonly used in luminescence dating and the ones used in this study (90–250 μm) travel as suspended load even in low flow due to their low Rouse numbers [*Rouse*, 1937] and low settling velocities [*Ferguson and Church*, 2004]. The Rouse number, R, is a nondimensional number that expresses the ratio of gravitational settling to turbulent upward momentum:

$$R = \frac{\omega_f}{k u_*} \tag{29}$$

where ω_f is the particle settling velocity, u_* is the shear velocity, and κ is von Karman's constant (0.41). For $R \geq 2.5$, sediment is dominantly bed load material; for $R = 2.5$–1.2, sediment is in partial suspension (saltation); for $R = 1.2$–0.8, sediment is in full suspension; and for $R < 0.8$, sediment travels as wash load with minimal chance of bed contact [*Rouse*, 1937]. Here we interpret suspended grains as those that take an extended distance of transport in between moments of contact with the bed. For a flow 1 m deep ($h = 1$), with a channel slope $S = 0.001$, a shear velocity calculated from the depth-slope product ($u_* = \sqrt{ghS}$), and settling velocities calculated from *Ferguson and Church* [2004], the coarsest grain size used in this study (250 μm) will have a Rouse number of approximately 0.8: well within the suspended range. As the depth of the flow or slope increases, or the grain size decreases, the Rouse number will only decrease as the flow is able to produce stronger turbulence. Furthermore, if we consider that the majority of sediment is transported in large floods which have significantly greater discharge than the annual flood [*Wolman and Miller*, 1960; *Nash*, 1994], the grain sizes used in this study (90–250 μm) should be considered as suspended sediment. Turbulence will cause grains to move throughout the water column [*Argall et al.*, 2004; *Man and Tsai*, 2007] with brief, but potentially frequent, exposure to light at the flow surface.

Because grains rapidly move from the bed to the surface of a flow, their bleaching history integrates periods of high-intensity, low spectral attenuation near the surface, to low-intensity, high spectral attenuation near the bed. The effect of turbulence on the bleaching rate was also observed by *Ditlefsen* [1992] and *Gemmell* [1985], where both witnessed a lowering in bleaching rate with increased turbulence, suggesting that turbulence brings more sediment into the flow and increases the water opacity despite also elevating grains closer to the surface. We cannot account for turbulent motion with the current bleaching experiment data of *McGuire and Rhodes* [2015a] because the experiment was not performed in turbid water. However, if we assume that the magnitude of light intensity is more important than the role of spectral attenuation on bleaching rate, then we can use equation (18) as a first-order approximation. Further research into the relative role of turbulence versus spectral filtering on bleaching rates would help to better evaluate this assumption. Finally, we assume that turbidity, represented by z_*, is constant. We base this on the expectation that the higher flows, during which large amounts of sediment are transported, will typically be turbid. However, we acknowledge that significant complexity exists with respect to turbidity [*Belmont et al.*, 2009] and its effect on luminescence bleaching [*Gemmell*, 1997] such that further study is warranted.

It is important to point out that the model provides a framework for understanding the general trend of the mean equivalent dose with increasing transport distance rather than the random fluctuations in equivalent dose potentially due to smaller-scale processes such as depositional mechanism across a point bar [*King et al.*, 2014a; *Cunningham et al.*, 2015a]. Although the model can be modified to include the effects of processes such as erosion of older terraces and tributary input with high stored-sediment luminescence, $\mathscr{L}_b$ (Figure 2), the potential effects of smaller scale processes must be considered. In an elucidative series of papers, *King et al.* [2013, 2014a, 2014b] found that for glaciofluvial braid-bar systems, the dispersion in luminescence measurements within a single bar could be greater than the change in luminescence downstream

over a 1–10 km study reach. We suggest that their data also imply that both the dispersion and magnitude of luminescence intensity decrease with distance, especially at reach-scale (10–100 km) transport distances, potentially consistent with the results of our model, although their sediment system was notably different from those considered here. *Cunningham et al.* [2015a] discovered a correlation with the proportion of bleached grains versus height above the low-flow water level for a South African bedrock river, which they interpreted as indicating deposition by large turbid floods, as opposed to clear water during low flows. However, significant scatter seems to be present when these variables are compared in the lower Rhine [*Cunningham et al.*, 2015b]. *Porat et al.* [2001] found that for a flash-flood-driven ephemeral river in southern Israel, the variability in equivalent dose within individual deposits obscured any potential downstream trend in their 800 m study reach. However, their suggestion that an 800 m reach is too small to see these trends is consistent with the parameters obtained during our application of the model, which demonstrates that downstream trends are apparent at the scale of tens of kilometers.

It should be noted that the model is here applied to all grains in the 90–250 μm range under the assumption that the bleaching rates across grain sizes is similar and that transport information across these sizes can be averaged. Grains in this range have been observed to have size-dependent residual doses in modern sediment [*Olley et al.*, 1998], with the interpretation that coarser grain sizes are generally better bleached than finer sizes [*Wallinga*, 2002; *Truelsen and Wallinga*, 2003; *Rittenour*, 2008]. This is counterintuitive as it would be expected that finer grain sizes undergo greater fluid suspension than coarse grains and should therefore be better bleached [*Wallinga*, 2002; *Rittenour*, 2008]. However, this observation may be explained by the finding that finer grain sizes tend to have higher exchange rates and shorter transport length scales than coarse grain sizes [*Lauer and Willenbring*, 2010]. This would mean that finer grain sizes have greater probability of being deposited in floodplains for longer periods and regenerating signal during deposition. The relative difference in sunlight exposure due to greater suspension of finer grains may actually be insignificant because all grains in the 90–250 range will have low Rouse numbers and greater time spent in fluid suspension during the large floods that move the majority of sediment [*Wolman and Miller*, 1960]. Another possibility is that the greater residual doses seen in finer grain sizes reflect differences in intrinsic bleachability of a luminescence signal at that grain size. *McGuire and Rhodes* [2015a] noted that bleaching experiments across the 125–250 μm grain size range seem to show consistent behavior such that characterizing the bulk bleaching behavior of grains in this range is sufficient for our purposes. Flume experimentation may be necessary to conclusively test whether potential processes such as clay flocculation [e.g., *Lepper*, 1995] lead to differential grain size bleaching rates in turbulent flow. However, bleaching rates do not currently seem to be a major source of uncertainty in our model results.

Finally, in order to use a luminescence signal for this method, the luminescence intensity or equivalent dose must decline in an approximate and consistent manner with progressive sunlight exposure. Signals such as OSL, IRSL, post-IR IRSL, MET-pIRIR, and thermoluminescence (TL) seem to follow this pattern sufficiently during sunlight bleaching experiments [*Reimann et al.*, 2015; *McGuire and Rhodes*, 2015a; *Colarossi et al.*, 2015]. The choice of luminescence signal may depend on the environment and the scale of interest. Fast-to-bleach signals, such as OSL, may bleach so rapidly that the mean equivalent dose is so close to zero that large uncertainties result in the derived sediment transport values. Slow-to-bleach signals, such as TL or high-temperature post-IR IRSL, may not rapidly reach steady state dose conditions (i.e., $\partial L/\partial x \approx 0$) due to changes in input sediment ($\mathscr{L}_b$) because of the longer distances needed to bleach sediment than easier to bleach signals (Figure 2). However, it is worth noting that slow-to-bleach signals may produce more consistent long-distance patterns as the faster bleaching rate of signals such as OSL can lead to large statistical dispersion under variable light exposure and greater intersample noise. Further research and experimentation will be needed to access which signal is appropriate for which environment. However, this may be an advantage as different MET-pIRIR signals could potentially allow one to "fine tune" for the environment of interest. Note that we do not include the possible influx of eolian sand which may cause the apparent bleaching rate in the river to be higher than estimated or measured in laboratory experiments, which would cause estimates of the transport velocity u to be faster than actual. However, as long as the flux of eolian sediment is not of large volume compared to the volume of river sediment, this should not be a problematic factor.

4.3. Sediment Residence Time and Characteristic Scales

A key advantage of this method is that both the characteristic lengthscale of transport, ℓ_s, and the characteristic time scale of storage, τ_s, can be estimated from the luminescence in-channel sediment and nearby

deposits. One of the central assumptions in the model is that both ℓ_s and τ_s of sediment transport can be captured by definable averages for the majority of grains. The model implements this assumption in two ways. The first is the assumption that the characteristic transport lengthscale, ℓ_s, accurately defines the distances average grains travel between depositions in long-term storage centers. The second assumption is that the time each grain spends in storage, the characteristic storage time scale, τ_s, can also be captured by a definable average. The assumption that these values can be adequately captured by averages rests on the probability distributions controlling sediment transport and sediment storage [*Furbish et al.*, 2012].

Sediment in transport is commonly thought of as an ensemble of particles that undergo periods of motion and periods of rest [*Furbish et al.*, 2012]. Probability distributions can be used to describe the stochastic nature of these sediment transport episodes, which together can be used to define the nature and virtual velocity of transport [*Haschenburger and Church*, 1998; *Bradley et al.*, 2010; *Furbish et al.*, 2012]. This concept can be found in studies of bed load transport [*Furbish et al.*, 2012; *Roseberry et al.*, 2012] and saltating particles in wind [*Anderson and Haff*, 1988; *Valance et al.*, 2015]. However, an understanding of the transport episodes of suspended sediment transport is lacking [*Parsons et al.*, 2015]. The probability distribution of transport distances for suspended sediment is uncertain, and it is debatable what the effects of different probability distributions would be on the mean equivalent dose of channel fine sand. Grains of sand in rivers should have greater cumulative sunlight exposure, and thus bleaching, with cumulative distance given that fluid turbulence should move the grain into the photic zone near the water surface repeatedly. This scaling of sunlight exposure with transport distance would mean that the decrease in luminescence for a grain should also scale with transport distance. However, this scaling breaks down if the grain becomes fully bleached. If the suspended sediment transport distance distribution favors long transport distances, grains will be advected without recording further transport distance. However, if the mean of the distance of transport distribution is short, then the scaling holds and this may support the characteristic transport lengthscale method used in the model. Whether a mean of transport distances can be captured by a luminescence signal depends on the signal's bleaching rate, with fast-to-bleach signals such as IR50 and quartz OSL having a higher probability of being completely removed before a transport episode of a grain ends. For this reason, slower-to-bleach luminescence signals are advantageous as they are more likely to capture the mean transport distances than faster-to-bleach signals. Note that in this framework, we consider only episodes of transport between long-term storage sites where significant signal regeneration can occur. This restricts our consideration to the transport distances during characteristic floods. Short rests on the streambed may not matter unless the water is sufficiently clear to allow bleaching at the bed. Further study of the influence of suspended sediment transport distance probability distributions on luminescence could be approached with particle-based modeling and single-grain measurements.

Our second assumption, that the characteristic storage time scale, τ_s, can be captured by a definable average, depends on the probability distribution of the long-term "rest" or storage times of fine sand in natural river systems. We assume that there exists some characteristic mean time scale of fine sand storage such that on average, a particle rests for this amount of time before the next episode of transport. This assumption is also used in many estimates of time-averaged sediment virtual velocity [*Pizzuto et al.*, 2014, and references therein] and is implicitly made in many studies that collect geochronologic samples from fluvial landforms and assume that the resultant age is representative of the landform. In counterpoint, the possibility exists that the distribution of fine-sand residence times are such that recently deposited fine sand has a greater probability of re-entrainment than fine sand that was deposited earlier, leading to a power law ("gambler's ruin") sediment residence time distributions [*Tsai et al.*, 2014]. Another possible effect is an "erosion hazard" function in which re-entrainment is most likely at shorter time scales and at the longest time scales as channels move back and forth between valley walls [*Bradley and Tucker*, 2013].

The effect of residence time distribution on the equivalent dose of channel fine sand would be expressed through modification of the basal sediment dose $\mathscr{D}_b$. If a channel reoccupies a location where it has recently deposited material, the $\mathscr{D}_b$ value will be lower due to smaller luminescence regeneration (say, tens to hundreds of years) than if the channel occupies a location that it had not occupied for a long time (say, hundreds to thousands of years) and significant luminescence regeneration occurred. The effect of floodplain residence-time distribution on the luminescence characteristics of channel sand deserves further study. The breadth and nature of this residence-time distribution should depend, among other things, on the sediment exchange rate, valley width, and channel migration rate [*Bradley and Tucker*, 2013]. Higher sediment

exchange rates and/or meandering rates will more likely allow the channel to reoccupy a previous location [*Lancaster and Casebeer*, 2007; *Lauer and Parker*, 2008b; *Wickert et al.*, 2013; *Limaye and Lamb*, 2016] and potentially move from one side of the valley back to the other. An additional complicating factor is that these rates may change with downstream distance [*Constantine et al.*, 2014], which would alter the probability distribution of storage times. Furthermore, an anastomosing system, such as a braided channel, may have different residence times and exchange rates for each channel braid, leading to further complications. As mentioned previously, particle-based numerical modeling may provide a way to assess the role of the sediment residence-time distribution. Furthermore, using a coupled landscape evolution and sediment transport model could provide insight into how processes such as a river meandering into older deposits may affect the pattern of channel equivalent dose.

4.4. Steady State Approximations and Geomorphic Disequilibrium

To apply the model for the field cases, we assume that the fine sand flux in the river channel, q_s, is constant in space and time over the study areas. This assumption allows for a direct application of the model without requiring additional information on the fine sand flux in the river in order to constrain transport velocity, u, and exchange rate, η. The assumption is, in effect, a statement that there are no significant spatial or temporal variations in the state of sediment supply of fine sand throughout a river system over the time scales relevant for fine sand transport from original erosional source to final depositional sink. These time scales are difficult to constrain, however, as storage times dominate the time a grain takes to cross from source to sink [*Pizzuto et al.*, 2014] and these storage times can span the range of hundreds to hundreds of thousands of years [*Lauer and Willenbring*, 2010]. We propose that the time scale of interest, τ_{system}, for this model is the expected time for a grain to travel the length of the river system, which is equal to the length of the river system, ℓ_{system}, divided by the virtual velocity, U:

$$\tau_{\text{system}} = \frac{\ell_{\text{system}}}{U} \tag{30}$$

Equation (30) shows how a longer river, or a lower virtual velocity, provides a larger time scale of integration. For the Mojave River study area, our estimated virtual velocity implies a time scale on the order of 10^4 years; for the Loire study area, the time scale is on the order of 10^5 years. As the time scale and lengthscales of the observed system increase, the assumption of a uniform sediment load becomes more tenuous. Nonetheless, our luminescence-derived virtual velocity estimates imply that the characteristic time scales for fine-sand transit in these two river systems integrate over a range of climate conditions, which is consistent with the findings of sediment-budget studies in other rivers [*Pizzuto et al.*, 2014, and references therein]. This indicates that the results presented here represent fine sand transport information (u, η, and derived values) averaged over a long period of time and potentially over periods of geomorphic transience. How this information is averaged over time by transport processes [*Willenbring et al.*, 2013] and whether/how changes in climate could affect our sediment transport values [*Jerolmack and Paola*, 2010; *Willenbring and von Blanckenburg*, 2010] remain significant research frontiers. However, we note that the assumptions involved in applying the model are not dissimilar to those used for analogous methods such as beryllium-derived catchment erosion rates, which form the basis for many successful studies [*Portenga and Bierman*, 2011, and references therein], or sediment transport modeling [*Lauer and Parker*, 2008a; *Lauer and Willenbring*, 2010; *Viparelli et al.*, 2013; *Belmont et al.*, 2014; *Pizzuto et al.*, 2014].

The presence of changing sediment loads, such as due to geomorphic landscape transience, does not necessarily invalidate the model. Rather, it requires that the additional information be taken into account in the theoretical framework. Observing a roughly constant luminescence value with downstream distance shows that a steady balance of bleaching and exchange is occurring and that these values can be quantified. Alternatively, if the luminescence versus downstream distance can be observed to be approximately increasing or decreasing, it may also be possible to quantify sediment transport information. Observations which show that large and frequent changes in the luminescence are occurring with downstream distance may indicate that the system is highly influenced by random influxes of unbleached/bleached sediment which would complicate a luminescence-based sediment transport analysis. Note that this observation is only relevant for samples taken in a consistent geomorphic location such as sediment taken deeper than 30 cm in channel bars. Sediment taken from banks may not be comparable with deep channel bar sediment or

shallow channel sediment and so forth. The general 1-D conservation law (equation (10)) allows for the possibility that fine-sand sediment load, q_s, varies in time and space. Likewise, the model can accommodate changes in the dose of eroded fine sand, as might be expected for a channel that erodes material of different ages in different reaches (Figure 2). For example, the Mojave River data set shows an increase in mean equivalent dose in the farthest downstream reaches of the channel (Figure 4e). This stretch of the river is characterized by an incised channel, and it receives water and sediment contributions from tributaries that have incised into alluvial fans. One might therefore expect an influx of material with a differing equivalent dose (new $\mathscr{L}_b$) into the main channel along this reach, which could explain the higher trapped charge concentration that we observe. If the $\mathscr{L}_b$ of the fine sand in the incised terraces were known, one could determine whether there is a difference in sediment-exchange rates within this incised reach as compared to the stable reaches upstream.

4.5. Implications for Sediment Transport Predictions

To conclude our points relevant to sediment transport predictions, we summarize them here. The first assumption is that the *majority* of bleaching of trapped charge occurs during fluvial transport. If this assumption were invalidated, there would be a large flux of bleached grains and the bulk bleaching of all grains in the river channel would be faster than expected by the model's use of and bleaching experiment data. This would cause an overestimation of the drift velocity u, the exchange rate η, and the virtual velocity U, proportionate to the relative amounts of surface bleached sediment versus transport bleached sediment. However, as noted above, this may not be a likely scenario. The second assumption, that characteristic transport and storage lengthscales and time scales for a river system have finite averages and/or variance, would affect the sediment transport predictions in the following ways. If the transport lengthscale has infinite mean, then the scaling relationship between the amount of luminescence bleached and the distance a grain travels breaks down and the luminescence of grains is no longer an effective proxy for the transport lengthscale. Studies of how sensitive river channel luminescence is with respect to different systems may lead to a better understanding on the controls of storage time scale and sediment transport. However, this may not be a problem for most river systems [*Bradley and Tucker*, 2013]. Infinite variance in the transport lengthscale is potentially avoided by measuring large numbers of grains as is done during luminescence measurement of large aliquots. Infinite mean in the storage time scale would mean that some grains in the system would mean that the scaling between the luminescence of the storage center deposits and the storage time breaks down as the grains become saturated with respect to luminescence. This would result in a underestimation of the storage time scale and an overestimation of the virtual velocity. This can be avoided by using a luminescence signal with a saturation limit higher than typical storage time scales such as the pIRIR signals used in the Mojave data set. As with the transport lengthscale, an infinite variance in the storage time scale can be potentially avoided by measuring large numbers of grains. The final two assumptions, that (a) steady state approximations are appropriate over suspended sediment transport time scales and (b) that no significant geomorphic disequilibria such as major changes in sediment supply are occurring over the time scales of fine sediment transport, vary in a complex manner. As discussed above, these assumptions may require that the model be modified for particular field sites in order to produce reasonable results. As with the application of analogous methods such as cosmogenic catchment-averaged denudation rates, the context of the state of the landscape will need to be considered with regard to these two assumptions.

As a final note, we return to the questions posed in the introduction. To help explain our answers to these questions, we craft a simplified analytical solution to the main equation (equation (11)). Under steady state conditions $\left(\frac{\partial \mathscr{L}}{\partial t} = 0\right)$ and when $\beta = 1$, equation (11) simplifies to

$$\mathscr{L}(x) = \mathscr{L}_0 e^{-\frac{k+\eta}{u}x} + \mathscr{L}_b \left[\frac{1 - e^{-\frac{k+\eta}{u}x}}{1 + \frac{k}{\eta}}\right] \tag{29}$$

and nondimensionalized as

$$\mathscr{L}^*(x) = e^{-\frac{x_0(k+\eta)}{u}x^*} + \frac{\mathscr{L}_b}{\mathscr{L}_0}\left[\frac{1 - e^{-\frac{x_0(k+\eta)}{u}x^*}}{1 + \frac{k}{\eta}}\right] \tag{30}$$

with $\mathscr{L}_0$ representing a starting upstream luminescence value and x_0 as a characteristic lengthscale such as a reach length. Equation (29) produces the basic form as presented in Figure 2. Note that the conditions needed to produce equation (29) may never happen in nature, but this equation provides a useful

conceptual demonstration. The first question is "what factors govern the rate of bleaching with respect to transport distance?" Our findings suggest that this rate depends on grain transport velocity (u), storage center exchange rate (η), and bleachability (k_t). This relationship can be seen in the above equation if we consider no storage center luminescence ($\mathscr{L}_b = 0$) and examine the preexponential term $\left(\frac{k+\eta}{u}\right)$. This term shows that an increase in the transport velocity u would cause a shallower gradient in $\mathscr{L}$ over downstream distance x. In contrast, an increase in the exchange rate (η) and/or bleachability (k_t) would cause a steeper gradient in $\mathscr{L}$ over the same downstream distance. The resulting effect serves to increase the distance that a higher or lower mean equivalent dose can be observed in channel sediment.

The second question is "why does sand sampled from channel deposits retain a signal even when the material is clearly subject to contemporary transport?" We find that under our theoretical conditions, an aliquot of sand from a channel should exhibit some signal because of sediment exchange between channel and storage (floodplains). Even at long transport distances, the signal seen in the downstream reaches should depend on exchange rate, luminescence equivalent dose of stored sediment, and bleachability (Figure 3). Equations (29) and (30) demonstrates this if the limit is taken as $x \to \infty$, which causes both exponential terms to go to zero such that $\mathscr{L}(x) = \frac{\mathscr{L}_b}{1+k/\eta}$. The in-channel luminescence, $\mathscr{L}$, is now only dependent on the storage center luminescence, $\mathscr{L}_b$; the bleachability, k; and the exchange rate, η. Unless there is a dependence of $\mathscr{L}_b$ on downstream distance, the luminescence with downstream distance will be constant. At large scales, such as at river lengths greater than 100 km, both $\mathscr{L}_b$ and η may show a dependence on downstream distance. Exploring this is beyond the scope of this study but presents opportunities for future research.

The last question is "to what extent do variations in luminescence along a river reflect transport dynamics, such as the rate of channel-floodplain exchange or the virtual velocity of grains?" We find that the luminescence along a river is sensitive to changes in sediment transport parameters such as the transport velocity (u) and exchange rate (η) based on (1) the model's ability to reproduce field data (Figures 4 and 5) through altering the values of u and η and (2) as demonstrated by the sensitivity analysis (Figure 6). This relationship between the luminescence and the as the transport velocity (u) and exchange rate (η) can also be observed in equations (29) and (30) above. These parameters also define the characteristic lengthscale and the virtual velocity, which suggests that luminescence may be a useful tool to extract these sediment transport parameters.

4.6. Future Research

For future applications and research, we propose a series of approaches. First, we recommend that the parameter L^* be determined empirically through bleaching experiments in natural sunlight. As noted previously, the Mojave River data set includes the bleaching experiments of *McGuire and Rhodes* [2015a], which allows for the surface value of f to be determined and does not require the extensive parameter estimation involved with the Loire data. The best case scenario would involve exposing river sediment with a known equivalent dose to sunlight conditions typical of sediment in active transport. Subaqueous bleaching experiments made at the effective depth of transport (see the supporting information) would provide a useful value of f and would help limit the assumptions necessary to produce a velocity estimate. We also recommend large numbers of samples taken from river sediment, as this would greatly improve the estimates of sediment transport. In particular, sample collection that focused on observing long-distance trends in $\partial \mathscr{L}/\partial x$ would improve results. Additional information on the luminescence of the eroding material $\mathscr{L}_b$ and sediment residence time probability $p(\tau_s)$ would further improve estimations. Particle-based numerical modeling incorporating sediment suspension and/or channel migration mechanics could provide an avenue to explore these effects. The detection and measurement of very slow to bleach luminescence signals may improve the utility of the model for larger-scale estimates of sediment transport. This model may also be applicable to fine silt (4–11 μm) which is also routinely used in luminescence dating. The advent of portable luminescence readers [*Sanderson and Murphy*, 2010] with gamma irradiation sensitivity-correction may mean that this luminescence data could be collected rapidly and cheaply in the field. This would cut down on the amount of time needed for often expensive field sediment budgeting campaigns and avoid problems that arise when large floods wash away tracer experiments. Overall, this method could improve research efficiency and provide an alternative method when others are not available or are less effective.

5. Conclusions

The model presented here demonstrates the potential of luminescence as a sediment transport indicator of fine sand. A simple model derived from conservation of energy (stored as luminescence) and conservation of mass (as sediment) can reproduce the downstream patterns of luminescence observed in two river systems, the Mojave River in Southern California, USA, and the Loire in southern France. Application of the model can produce estimates of characteristic transport length and time scales, storage-center exchange rates, and time-averaged virtual velocity. The estimates made from the Mojave and Loire data sets appear to show a larger range than previously observed, but this may not be surprising considering the differences in river morphology from the previously published results. The model requires a series of assumptions that may or may not be valid in all circumstances and must be considered thoroughly, and properly accommodated when possible. However, deviations from the expected steady state conditions described by the model may help locate and interpret geomorphic disequilibrium. This study indicates that luminescence may hold significant utility toward obtaining sediment transport information from river systems and provides a potential new method to collect these data.

Notation List: Variable Units and Descriptions

Symbol	Units	Description
D_*	J/kg	dose growth parameter
D_E	J/kg	equivalent dose
D_R	J/kg/yr	background environmental dose rate
f	s^{-1}	loss rate of integrated luminescence intensity
f_D	s^{-1}	fraction of suspended sediment flux deposited per second during transport
f_E	s^{-1}	fraction of suspended sediment flux entrained from storage per second during transport
f_o	s^{-1}	unattenuated bleaching rate of integrated luminescence intensity
h	m	height of control volume
I_0	arbitrary units (luminescence)	initial sensitivity-corrected integrated luminescence intensity
I_{sat}	arbitrary units (luminescence)	sensitivity-corrected integrated luminescence intensity at saturation
k_t	s^{-1}	loss rate of equivalent dose with sunlight exposure
$\mathscr{L}$	J/kg	mean equivalent dose of sediment at a given point in the river channel
$\mathscr{L}^\circ$	J/kg/s	term describing change in channel mean luminescence as a function of exchange with a storage center
$\mathscr{L}^*$	J/kg/s	loss rate of equivalent dose due to sunlight exposure
ℓ_s	m	characteristic lengthscale in channel where most traveling particles have been deposited in long-term storage
ℓ_{system}	m	lengthscale of a system of interest
$\mathscr{L}_b$	J/kg	mean equivalent dose of sediment in storage centers accessible by the channel.
N_e	J	number of trapped electrons in a control volume
Q	J/kg	flux term describing movement of sediment with equivalent dose L
q_s	m^3/s	sediment flux
t_s	yr	time fine sand spends in long-term storage
u	m/s	transport velocity of suspended sediment
U	m/yr	time-averaged virtual velocity
w	m	width of control volume
x	m	downstream distance
z_*	m	light attenuation coefficient representing water turbidity
z_{eff}	m	effective depth in which a stationary grain will receive equal amounts of sunlight as a grain in turbulence (see the supporting information)
β	nondimensional	decay order of luminescence signal of interest
γ	cm^2/photons	variable relating equivalent dose or luminescence intensity versus
η	s^{-1}	channel sediment/long-term storage center exchange rate
λ	nm	wavelength of a single color of light
τ_s	year	characteristic time scale of long-term sediment storage
τ_{system}	year	time scale of a system of interest
φ	photons/cm^2/nm/s	photon flux for a given wavelength per second per cross-sectional area
φ_0	photons/cm^2/nm/s	photon flux prior to attenuation by water

Acknowledgments

We would like to thank Nathan Brown, Daniel Hobley, Amanda Keen-Zebert, Rachel Glade, and Charlie Shobe for constructive discussions. Thank you to Mayank Jain, Andrew Murray, Andrew Cyr, and Katherine Skalak for constructive comments on earlier versions of this manuscript. Thank you to Editors John Buffington and Mikael Attal and three anonymous reviewers for comments which greatly improved the manuscript. H.J.G. was supported by a Center for Integrative Research in Environmental Sciences (CIRES) fellowship. Any use of trade, product, or firm names is for descriptive purposes only and does not imply endorsement by the U.S. Government. The data used in this paper are referenced in the text. We are grateful for the support from the National Science Foundation (EAR-1246546).

References

Anderson, R. S., and P. K. Haff (1988), Simulation of eolian saltation, *Science*, *241*(4867), 820–823.

Argall, R., B. F. Sanders, and Y. K. Poon (2004), Random-walk suspended sediment transport and settling model, in *Estuarine and Coastal Modeling*, *Eighth Int. Conf.*, pp. 713–730, Am. Soc. of Civil Engineers, Monterey, Calif.

Bailey, R. M., B. W. Smith, and E. J. Rhodes (1997), Partial bleaching and the decay form characteristics of quartz OSL, *Radiat. Meas.*, *27*(2), 123–136.

Bailey, R. M., E. G. Yukihara, and S. W. S. McKeever (2011), Separation of quartz optically stimulated luminescence components using green (525 nm) stimulation, *Radiat. Meas.*, *46*(8), 643–648.

Belmont, P., D. P. Morris, F. J. Pazzaglia, and S. C. Peters (2009), Penetration of ultraviolet radiation in streams of eastern Pennsylvania: Topographic controls and the role of suspended particulates, *Aquat. Sci.*, *71*(2), 189–201.

Belmont, P., J. K. Willenbring, S. P. Schottler, J. Marquard, K. Kumarasamy, and J. M. Hemmis (2014), Toward generalizable sediment fingerprinting with tracers that are conservative and nonconservative over sediment routing timescales, *J. Soils Sediments*, *14*(8), 1479–1492.

Bradley, D. N., and G. E. Tucker (2012), Measuring gravel transport and dispersion in a mountain river using passive radio tracers, *Earth Surf. Processes Landforms*, *37*(10), 1034–1045.

Bradley, D. N., and G. E. Tucker (2013), The storage time, age, and erosion hazard of laterally accreted sediment on the floodplain of a simulated meandering river, *J. Geophys. Res. Earth Surf.*, *118*, 1308–1319, doi:10.1002/jgrf.20083.

Bradley, D. N., G. E. Tucker, and D. A. Benson (2010), Fractional dispersion in a sand bed river, *J. Geophys. Res.*, *115*, F00A09, doi:10.1029/2009JF001268.

Buylaert, J. P., A. S. Murray, K. J. Thomsen, and M. Jain (2009), Testing the potential of an elevated temperature IRSL signal from K-feldspar, *Radiat. Meas.*, *44*(5), 560–565.

Colarossi, D., G. A. T. Duller, H. M. Roberts, S. Tooth, and R. Lyons (2015), Comparison of paired quartz OSL and feldspar post-IR IRSL dose distributions in poorly bleached fluvial sediments from South Africa, *Quat. Geochronol.*, *30*, 233–238.

Colls, A. E., S. Stokes, M. D. Blum, and E. Straffin (2001), Age limits on the Late Quaternary evolution of the upper Loire, *Quat. Sci. Rev.*, *20*(5), 743–750.

Constantine, J. A., T. Dunne, J. Ahmed, C. Legleiter, and E. D. Lazarus (2014), Sediment supply as a driver of river meandering and floodplain evolution in the Amazon Basin, *Nat. Geosci.*, *7*(12), 899–903.

Cunningham, A. C., M. Evans, and J. Knight (2015a), Quantifying bleaching for zero-age fluvial sediment: A Bayesian approach, *Radiat. Meas.*, *81*, 55–61.

Cunningham, A. C., J. Wallinga, N. Hobo, A. J. Versendaal, B. Makaske, and H. Middelkoop (2015b), Re-evaluating luminescence burial doses and bleaching of fluvial deposits using Bayesian computational statistics, *Earth Surf. Dyn.*, *3*(1), 55–65.

Davies-Colley, R. J., and D. G. Smith (2001), Turbidity, suspended sediment, and water clarity: A review, *J. Am. Water Res. Assoc.*, *37*, 1085–1101, doi:10.1111/j.1752-1688.2001.tb03624.

Davies-Colley, R. J., and J. W. Nagels (2008), Predicting light penetration into river waters, *J. Geophys. Res.*, *113*, G03028, doi:10.1029/2008JG000722.

Ditlefsen, C. (1992), Bleaching of K-feldspars in turbid water suspensions: A comparison of photo-and thermoluminescence signals, *Quat. Sci. Rev.*, *11*(1), 33–38.

Ferguson, R. I., and M. Church (2004), A simple universal equation for grain settling velocity, *J. Sediment. Res.*, *74*(6), 933–937.

Furbish, D. J., P. K. Haff, J. C. Roseberry, and M. W. Schmeeckle (2012), A probabilistic description of the bed load sediment flux: 1. Theory, *J. Geophys. Res.*, *117*, F03031, doi:10.1029/2012JF002352.

Gemmell, A. M. (1997), Fluctuations in the thermoluminescence signal of suspended sediment in an alpine glacial meltwater stream, *Quat. Sci. Rev.*, *16*(3), 281–290.

Gemmell, A. M. D. (1985), Zeroing of the TL signal of sediment undergoing fluvial transportation: A laboratory experiment, *Nucl. Tracks Radiat. Meas.*, *10*(4), 695–702.

Gray, H. J., and S. A. Mahan (2015), Variables and potential models for the bleaching of luminescence signals in fluvial environments, *Quat. Int.*, *362*, 42–49.

Haschenburger, J. K., and M. Church (1998), Bed material transport estimated from the virtual velocity of sediment, *Earth Surf. Processes Landforms*, *23*(9), 791–808.

Hassan, M. A., M. Church, and P. J. Ashworth (1992), Virtual rate and mean distance of travel of individual clasts in gravel-bed channels, *Earth Surf. Processes Landforms*, *17*(6), 617–627.

Huntley, D. J., D. I. Godfrey-Smith, and M. L. Thewalt (1985), Optical dating of sediments, *Nature*, *313*, 105–107.

Idso, S. B., and R. G. Gilbert (1974), On the universality of the Poole and Atkins Secchi disk-light extinction equation, *J. Appl. Ecol.*, *11*(1), 399–401.

Jain, M., A. S. Murray, and L. Bøtter-Jensen (2003), Characterisation of blue-light stimulated luminescence components in different quartz samples: Implications for dose measurement, *Radiat. Meas.*, *37*(4), 441–449.

Jain, M., A. S. Murray, and L. Botter-Jensen (2004), Optically stimulated luminescence dating: How significant is incomplete light exposure in fluvial environments?, *Quaternaire*, *15*(1), 143–157.

Jerolmack, D. J., and C. Paola (2010), Shredding of environmental signals by sediment transport, *Geophys. Res. Lett.*, *37*, L19401, doi:10.1029/2010GL044638.

Julian, J. P., M. W. Doyle, and E. H. Stanley (2008), Empirical modeling of light availability in rivers, *J. Geophys. Res.*, *113*, G03022, doi:10.1029/2007JG000601.

Kars, R. H., T. Reimann, C. Ankjærgaard, and J. Wallinga (2014), Bleaching of the post-IR IRSL signal: New insights for feldspar luminescence dating, *Boreas*, *43*(4), 780–791.

King, G. E., R. A. J. Robinson, and A. A. Finch (2013), Apparent OSL ages of modern deposits from Fåbergstølsdalen, Norway: Implications for sampling glacial sediments, *J. Quat. Sci.*, *28*(7), 673–682.

King, G. E., D. C. Sanderson, R. A. Robinson, and A. A. Finch (2014a), Understanding processes of sediment bleaching in glacial settings using a portable OSL reader, *Boreas*, *43*(4), 955–972.

King, G. E., R. A. J. Robinson, and A. A. Finch (2014b), Towards successful OSL sampling strategies in glacial environments: Deciphering the influence of depositional processes on bleaching of modern glacial sediments from Jostedalen, Southern Norway, *Quat. Sci. Rev.*, *89*, 94–107.

Lancaster, S. T., and N. E. Casebeer (2007), Sediment storage and evacuation in headwater valleys at the transition between debris-flow and fluvial processes, *Geology*, *35*(11), 1027–1030.

Lauer, J., and G. Parker (2008a), Modeling framework for sediment deposition, storage, and evacuation in the floodplain of a meandering river: Theory, *Water Resour. Res.*, *44*, W04425, doi:10.1029/2006WR005528.
Lauer, J., and J. Willenbring (2010), Steady state reach-scale theory for radioactive tracer concentration in a simple channel/floodplain system, *J. Geophys. Res.*, *115*, F04018, doi:10.1029/2009JF001480.
Lauer, J. W., and G. Parker (2008b), Net local removal of floodplain sediment by river meander migration, *Geomorphology*, *96*(1), 123–149.
Leopold, L. B., W. W. Emmett, and R. M. Myrick (1966), Channel and hillslope processes in a semiarid area, New Mexico, Professional Paper 352-G. U.S. Geol. Surv. p. 193–253
Lepper, K. E. (1995), The effect of turbidity on the solar resetting of the luminescence signal: Implications for luminescence geochronology, Undergraduate Honors Thesis, The Ohio State Univ.
Li, B., and S. H. Li (2011), Luminescence dating of K-feldspar from sediments: A protocol without anomalous fading correction, *Quat. Geochronol.*, *6*(5), 468–479.
Limaye, A. B. S., and M. P. Lamb (2016), Numerical model predictions of autogenic fluvial terraces and comparison to climate change expectations, *J. Geophys. Res. Earth Surf.*, *121*, 512–544, doi:10.1002/2014JF003392.
Lu, J. Y., C. C. Su, J. H. Hong, and E. J. Chen (2012), Prediction of maximum general scour depth during a flood for intermittent rivers, in Proceedings of 6th International Conference on Scour and Erosion, pp. 27–31.
Man, C., and C. W. Tsai (2007), Stochastic partial differential equation-based model for suspended sediment transport in surface water flows, *J. Eng. Mech.*, *133*(4), 422–430.
Martin, Y., and M. Church (2004), Numerical modelling of landscape evolution: Geomorphological perspectives, *Prog. Phys. Geogr.*, *28*(3), 317–339.
McGuire, C., and E. J. Rhodes (2015a), Determining fluvial sediment virtual velocity on the Mojave River using K-feldspar IRSL: Initial assessment, *Quat. Int.*, *362*, 124–131.
McGuire, C., and E. J. Rhodes (2015b), Downstream MET-IRSL single-grain distributions in the Mojave River, southern California: Testing assumptions of a virtual velocity model, *Quat. Geochron.*, *30*, 239–244.
Meade, R. H. (2007), Transcontinental moving and storage: The Orinoco and Amazon Rivers transfer the Andes to the Atlantic, in *Large Rivers: Geomorphology and Management*, edited by A. Gupta, pp. 45–64, John Wiley, Chichester, U. K.
Murray, A. S., and A. G. Wintle (2000), Luminescence dating of quartz using an improved single-aliquot regenerative-dose protocol, *Radiat. Meas.*, *32*(1), 57–73.
Murray, A., J. P. Buylaert, and C. Thiel (2015), A luminescence dating intercomparison based on a Danish beach-ridge sand, *Radiat. Meas.*, *81*, 32–38.
Nash, D. B. (1994), Effective sediment-transporting discharge from magnitude-frequency analysis, *J. Geol.*, *105*(1), 79–95.
Olley, J., G. Caitcheon, and A. Murray (1998), The distribution of apparent dose as determined by optically stimulated luminescence in small aliquots of fluvial quartz: Implications for dating young sediments, *Quat. Sci. Rev.*, *17*(11), 1033–1040.
Papanicolaou, A. N., M. Elhakeem, G. Krallis, S. Prakash, and J. Edinger (2008), Sediment transport modeling review—Current and future developments, *J. Hydraulic Eng.*, *134*(1), 1–14.
Parsons, A. J., J. Cooper, and J. Wainwright (2015), What is suspended sediment?, *Earth Surf. Processes Landforms*, *40*, 1417–1420, doi:10.1002/esp.3730.
Pietsch, T. J., J. M. Olley, and G. C. Nanson (2008), Fluvial transport as a natural luminescence sensitiser of quartz, *Quat. Geochronol.*, *3*(4), 365–376.
Pizzuto, J., et al. (2014), Characteristic lengthscales and time-averaged transport velocities of suspended sediment in the mid-Atlantic Region, USA, *Water Resour. Res.*, *50*, 790–805, doi:10.1002/2013WR014485.
Pizzuto, J., J. Keeler, K. Skalak, and D. Karwan (2016), Storage filters upland suspended sediment signals delivered from watersheds, *Geology*, *45*, 151–154.
Porat, N., E. Zilberman, R. Amit, and Y. Enzel (2001), Residual ages of modern sediments in an hyperarid region, Israel, *Quat. Sci. Rev.*, *20*(5), 795–798.
Portenga, E. W., and P. R. Bierman (2011), Understanding Earth's eroding surface with 10 Be, *GSA Today*, *21*(8), 4–10.
Reimann, T., P. D. Notenboom, M. A. De Schipper, and J. Wallinga (2015), Testing for sufficient signal resetting during sediment transport using a polymineral multiple-signal luminescence approach, *Quat. Geochronol.*, *25*, 26–36.
Rhodes, E. J. (2011), Optically stimulated luminescence dating of sediments over the past 200,000 years, *Annual Rev. Earth Planet. Sci.*, *39*, 461–488.
Rhodes, E. J. (2015), Dating sediments using potassium feldspar single-grain IRSL: Initial methodological considerations, *Quat. Int.*, *362*, 14–22.
Rittenour, T. M. (2008), Luminescence dating of fluvial deposits: Applications to geomorphic, palaeoseismic and archaeological research, *Boreas*, *37*(4), 613–635.
Roseberry, J. C., M. W. Schmeeckle, and D. J. Furbish (2012), A probabilistic description of the bed load sediment flux: 2. Particle activity and motions, *J. Geophys. Res.*, *117*, F03032, doi:10.1029/2012JF002353.
Rouse, H. (1937), Modern conceptions of the mechanics of sediment suspension, *Trans. ASCE*, *102*, 463–543.
Sanderson, D. C., and S. Murphy (2010), Using simple portable OSL measurements and laboratory characterisation to help understand complex and heterogeneous sediment sequences for luminescence dating, *Quat. Geochronol.*, *5*(2), 299–305.
Sanderson, D. C., P. Bishop, M. Stark, S. Alexander, and D. Penny (2007), Luminescence dating of canal sediments from Angkor Borei, Mekong Delta, southern Cambodia, *Quat. Geochronol.*, *2*(1), 322–329.
Singarayer, J. S., and R. M. Bailey (2004), Component-resolved bleaching spectra of quartz optically stimulated luminescence: Preliminary results and implications for dating, *Radiat. Meas.*, *38*(1), 111–118.
Sohbati, R., M. Jain, and A. Murray (2012), Surface exposure dating of non-terrestrial bodies using optically stimulated luminescence: A new method, *Icarus*, *221*(1), 160–166.
Stokes, S., H. E. Bray, and M. D. Blum (2001), Optical resetting in large drainage basins: Tests of zeroing assumptions using single-aliquot procedures, *Quat. Sci. Rev.*, *20*(5), 879–885.
Syvitski, J. P., C. J. Vörösmarty, A. J. Kettner, and P. Green (2005), Impact of humans on the flux of terrestrial sediment to the global coastal ocean, *Science*, *308*(5720), 376–380.
Thomsen, K. J., A. S. Murray, M. Jain, and L. Bøtter-Jensen (2008), Laboratory fading rates of various luminescence signals from feldspar-rich sediment extracts, *Radiat. Meas.*, *43*(9), 1474–1486.
Truelsen, J. L., and J. A. K. O. B. Wallinga (2003), Zeroing of the OSL signal as a function of grain size: Investigating bleaching and thermal transfer for a young fluvial sample, *Geochronometria*, *22*(1), e8.
Tsai, C. W., Y. Hsu, K. C. Lai, and N. K. Wu (2014), Application of gambler's ruin model to sediment transport problems, *J. Hydrol.*, *510*, 197–207.

Tucker, G. E., and G. R. Hancock (2010), Modelling landscape evolution, *Earth Surf. Processes Landforms*, *35*(1), 28–50.
Valance, A., K. R. Rasmussen, A. O. El Moctar, and P. Dupont (2015), The physics of Aeolian sand transport, *Comptes Rendus Phys.*, *16*(1), 105–117.
Van Rijn, L. C. (1993), *Principles of Sediment Transport in Rivers, Estuaries and Coastal Seas*, vol. 1006, Aqua publications, Amsterdam.
Viparelli, E., J. W. Lauer, P. Belmont, and G. Parker (2013), A numerical model to develop long-term sediment budgets using isotopic sediment fingerprints, *Comput. Geosci.*, *53*, 114–122.
Wallinga, J. (2002), Optically stimulated luminescence dating of fluvial deposits: A review, *Boreas*, *31*(4), 303–322.
Wickert, A. D., J. M. Martin, M. Tal, W. Kim, B. Sheets, and C. Paola (2013), River channel lateral mobility: metrics, time scales, and controls, *J. Geophys. Res. Earth Surf.*, *118*, 396–412, doi:10.1029/2012JF002386.
Willenbring, J. K., and F. von Blanckenburg (2010), Long-term stability of global erosion rates and weathering during late-Cenozoic cooling, *Nature*, *465*(7295), 211–214.
Willenbring, J. K., N. M. Gasparini, B. T. Crosby, and G. Brocard (2013), What does a mean mean? The temporal evolution of detrital cosmogenic denudation rates in a transient landscape, *Geology*, *41*(12), 1215–1218.
Wolman, M. G., and J. P. Miller (1960), Magnitude and frequency of forces in geomorphic processes, *J. Geol.*, *68*(1), 54–74.